



Jet discrimination with a quantum complete graph neural network

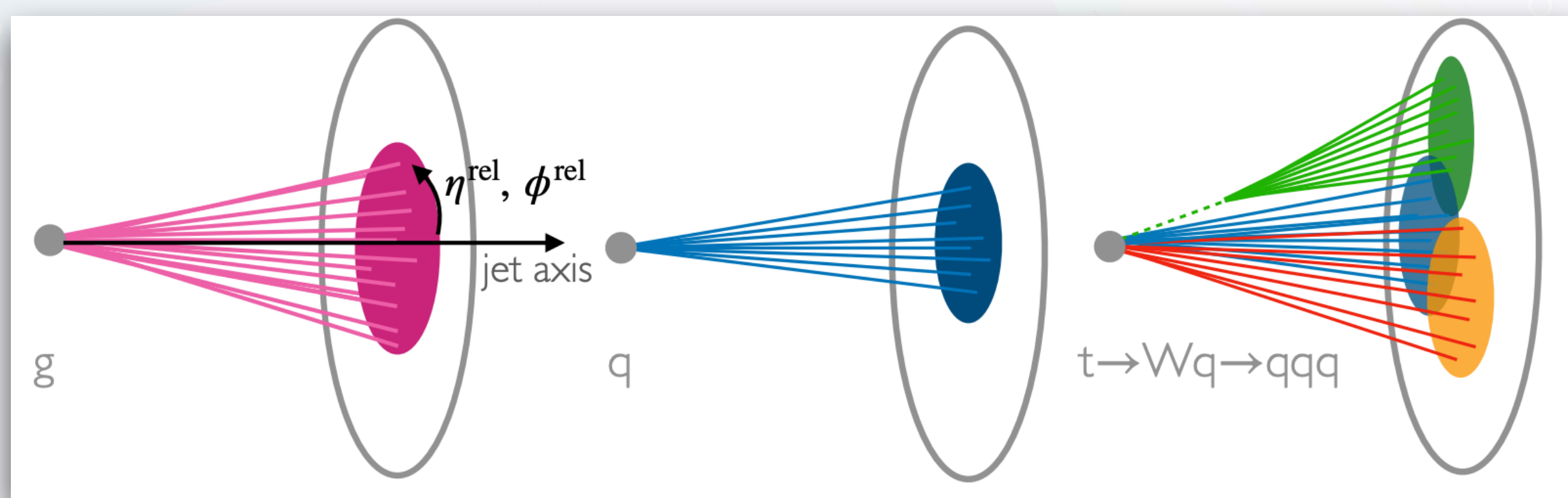
Yi-An Chen, Kai-Feng Chen

Department of Physics, National Taiwan University, Taipei, Taiwan

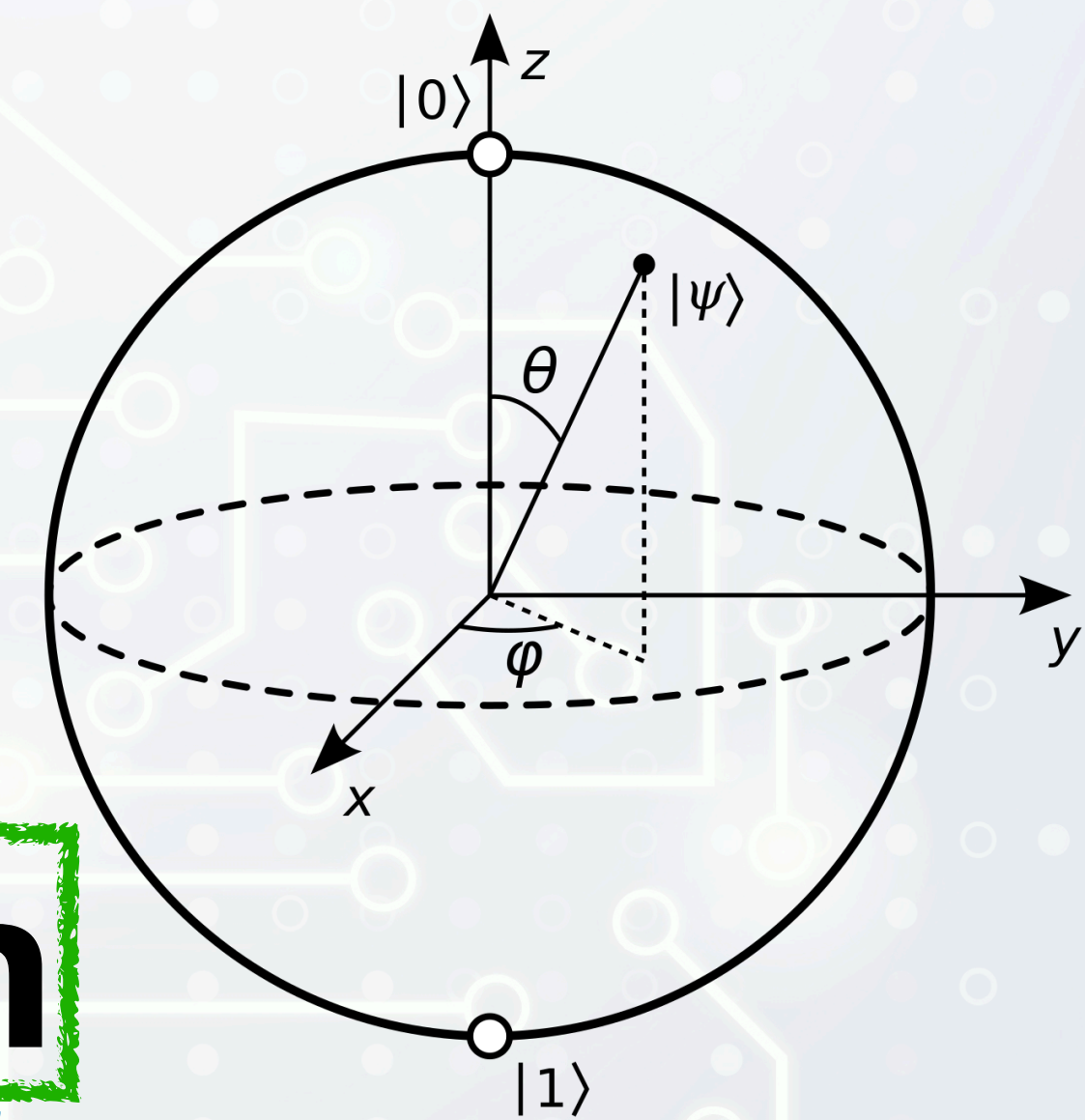
arXiv:2403.04990

Phys. Rev. D 111, 016020

March 18, 2025 ISGC @ Academia Sinica

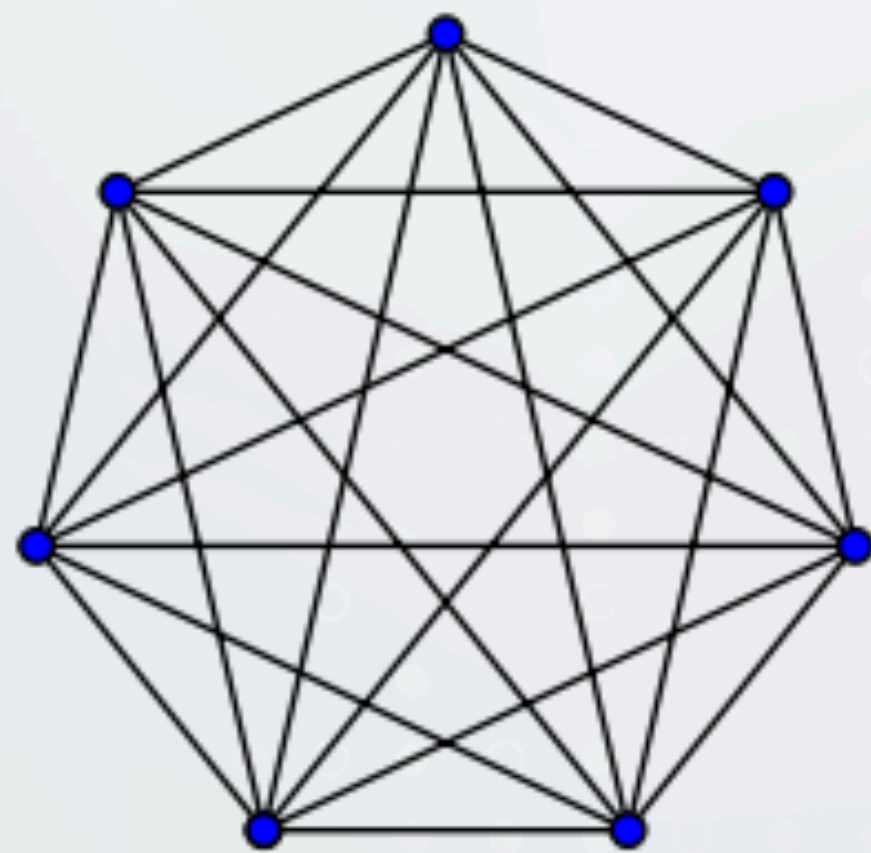


Jets, adapted from (arxiv 2106.11535)

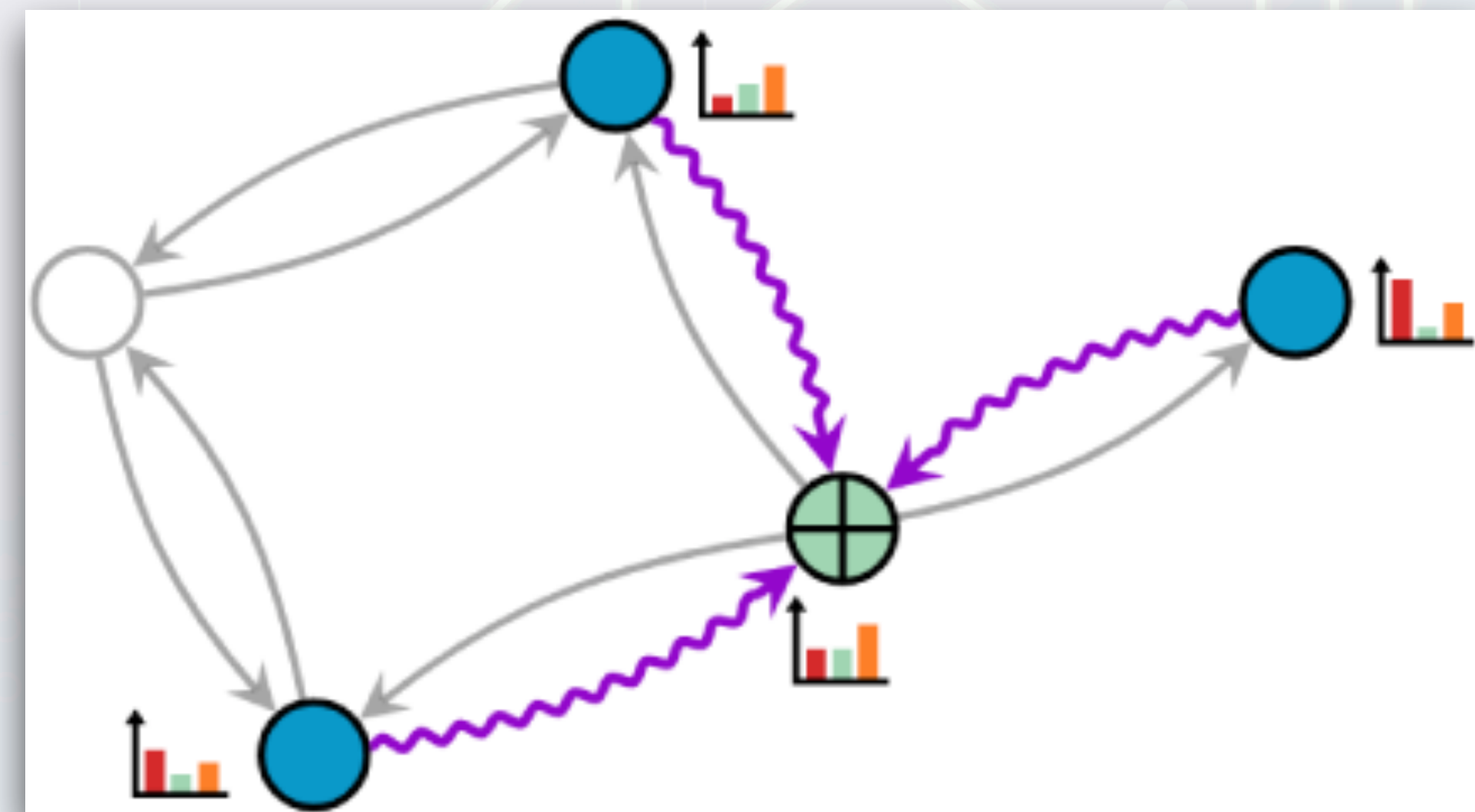


Bloch Sphere
(Adapted from Wikipedia)

Jet discrimination with a quantum complete graph neural network



Complete Graph
(Adapted from Wikipedia)



GNN (adapted from [PyTorch-Geometric](#))

Outline

- **Classical Machine Learning**
 - Message-Passing Graph Neural Network
- **Quantum Machine Learning**
 - Variational Quantum Circuit
 - **Quantum Complete Graph Neural Network**
- **Training X IBMQ X Summary**
 - Public Monte Carlo Simulated Jet Data
 - Running on IBMQ

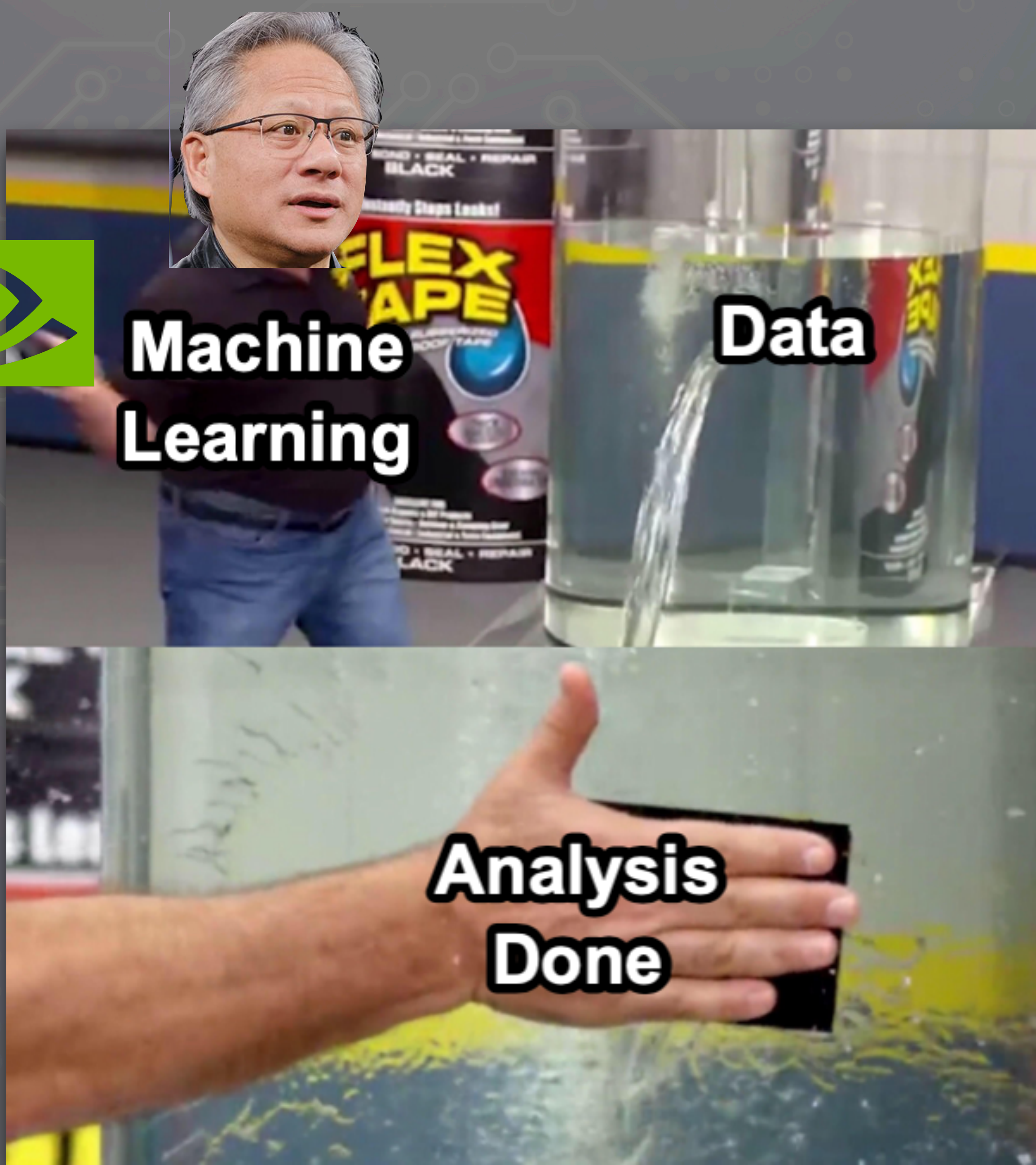


New
Quantum
Algorithm

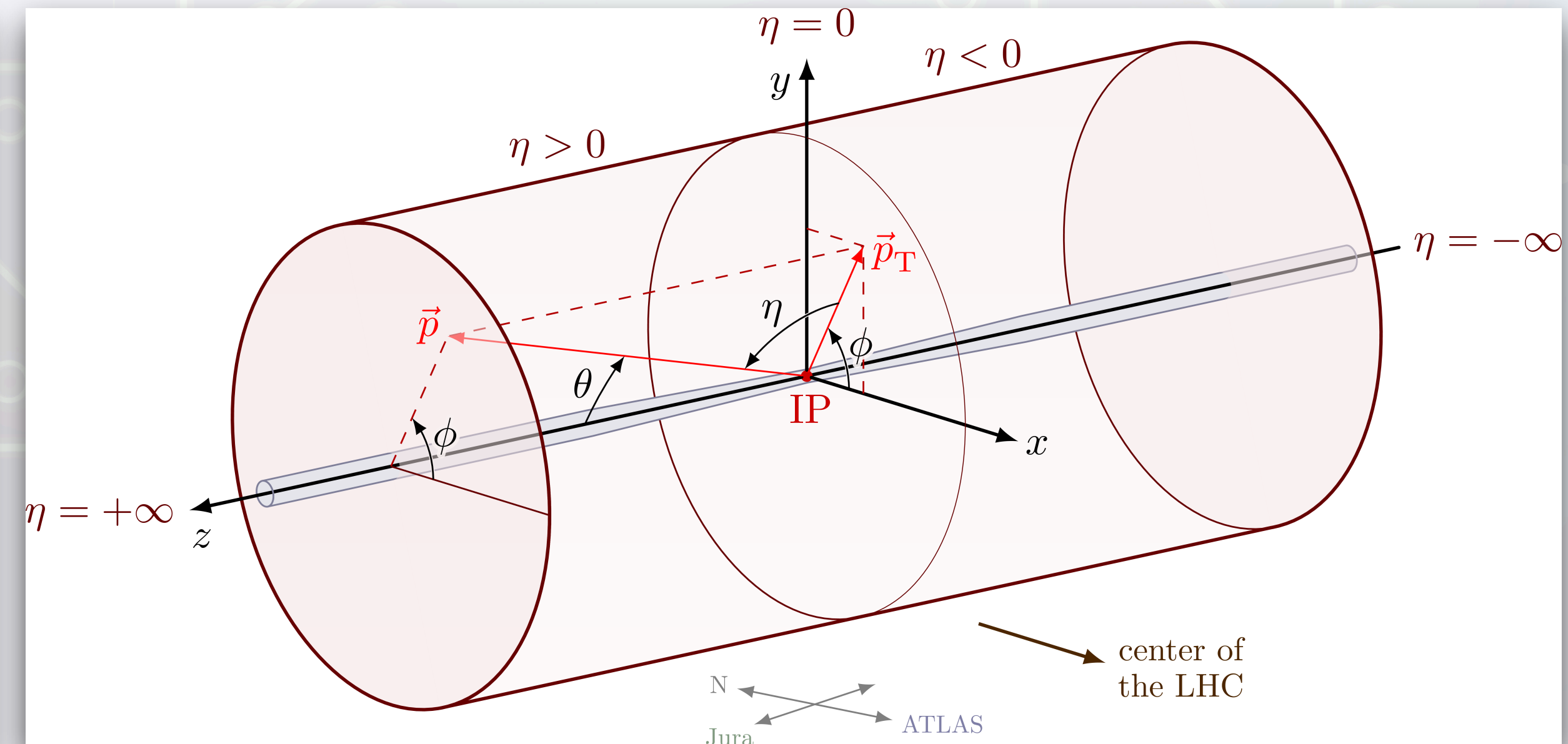
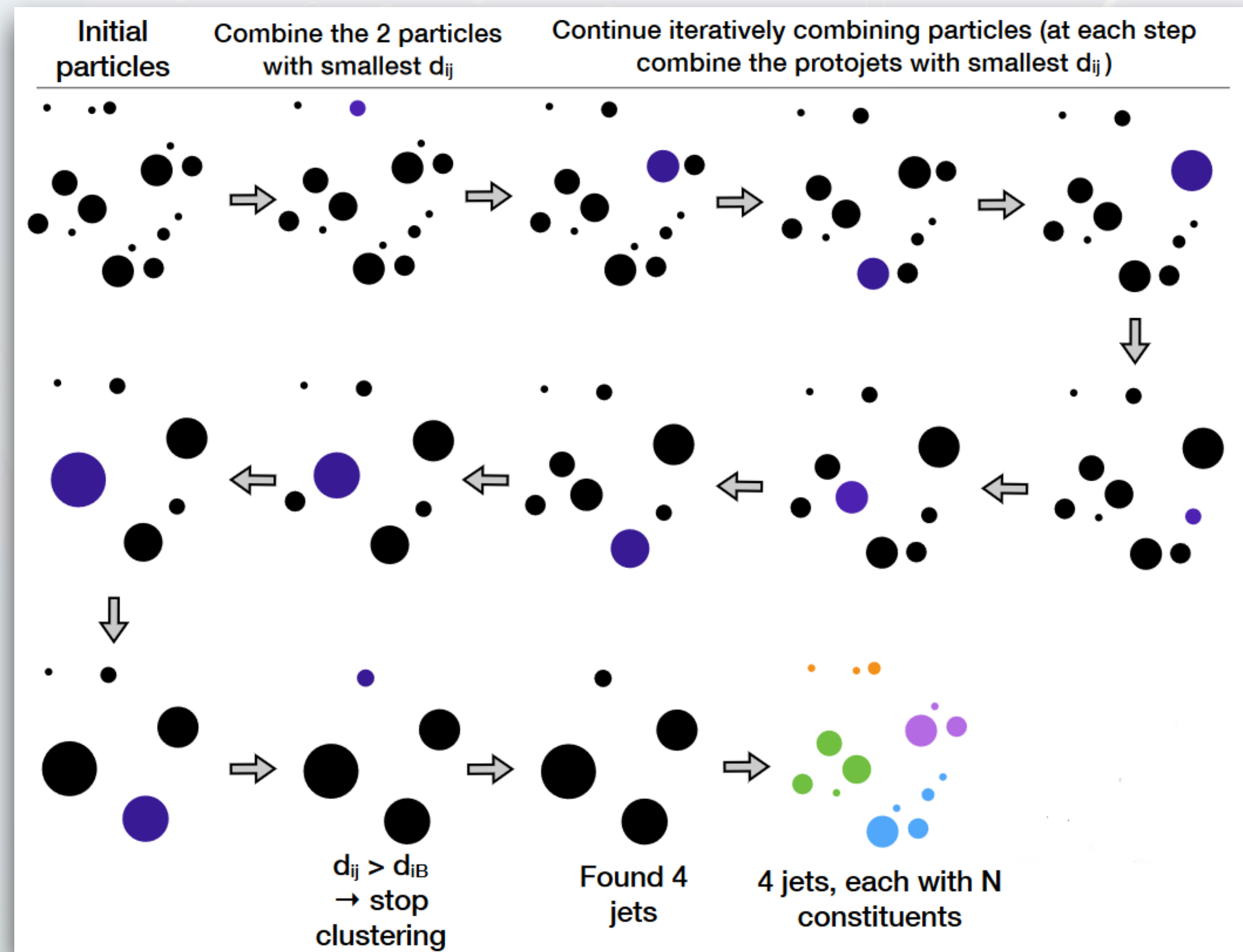


Variational
Quantum
Algorithm

Classical Neural Networks Models for Jet Discrimination



Jet Dataset



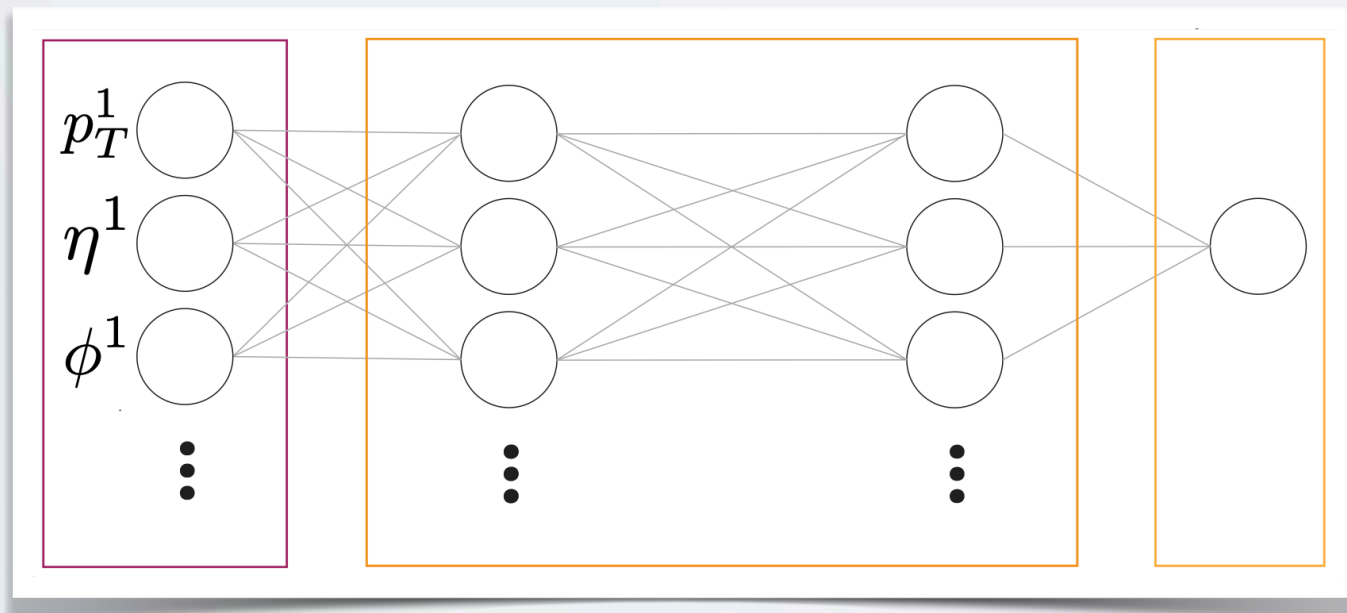
CMS Coordinate System by [Izaak Neutelings](#)

$$\vec{x} = (p_T, \Delta\eta, \Delta\phi)$$

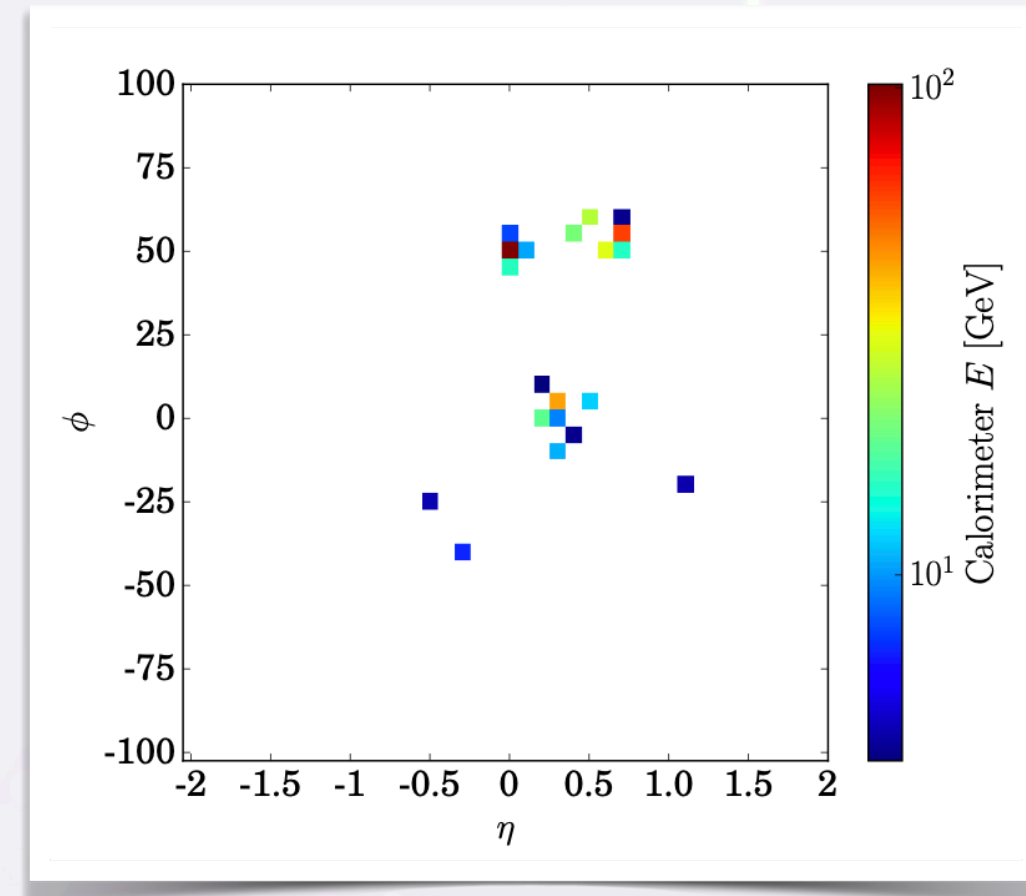
Figure adapted from 2021 [CMS Open Data Workshop](#)

Classical ML for Jets

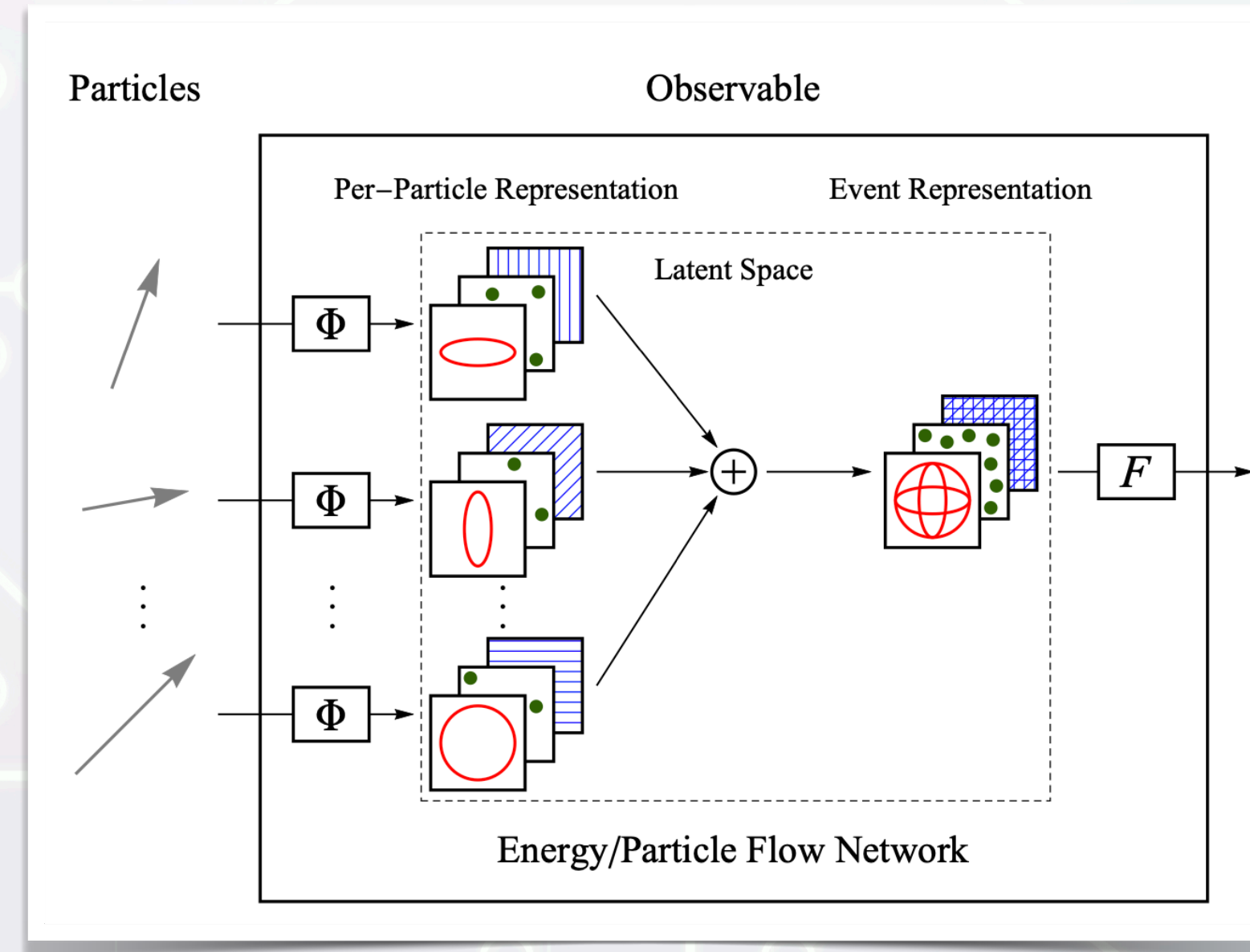
Overview



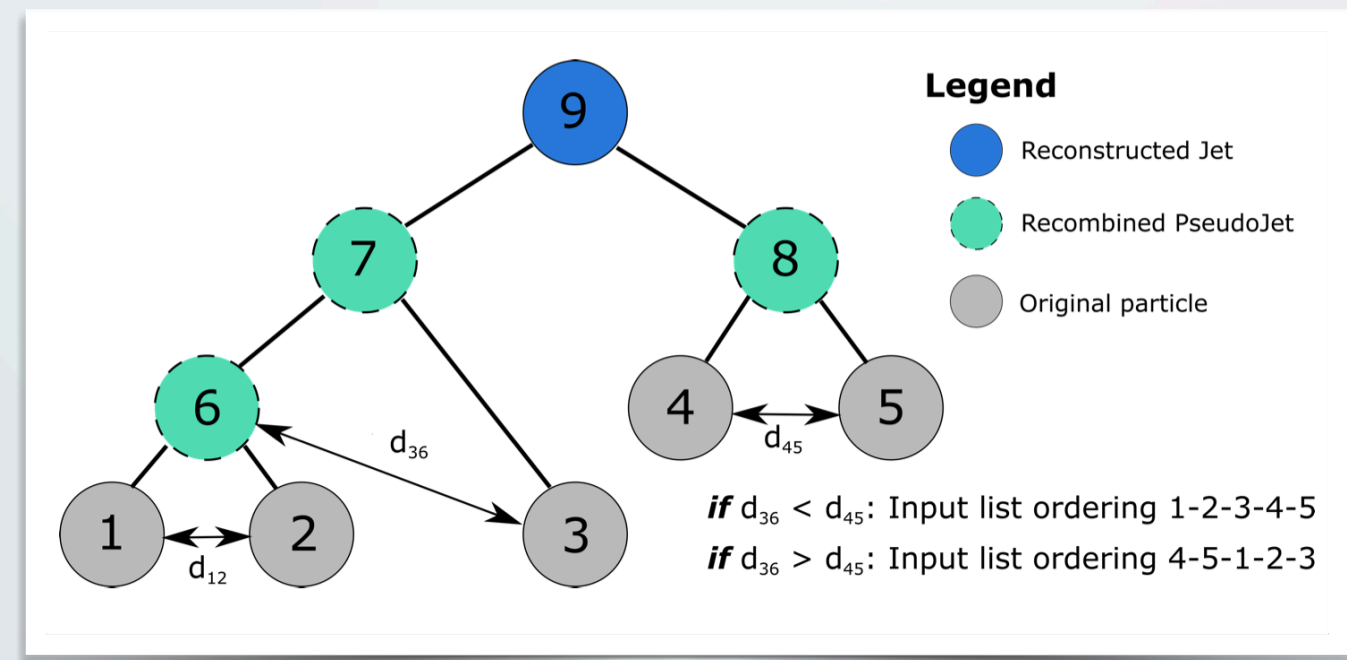
DNN (arXiv 1704.02124)



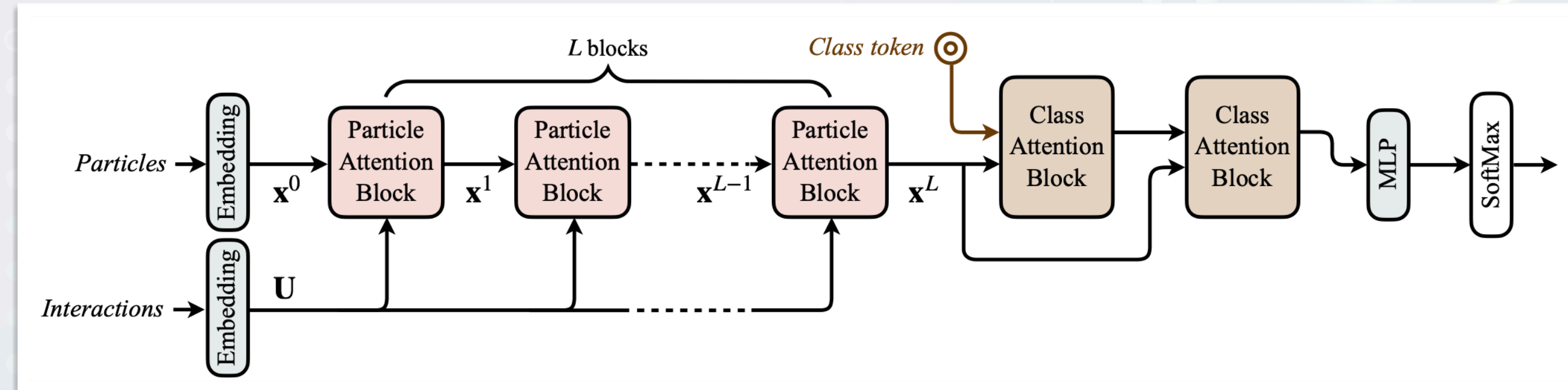
CNN (arXiv 1707.08966)



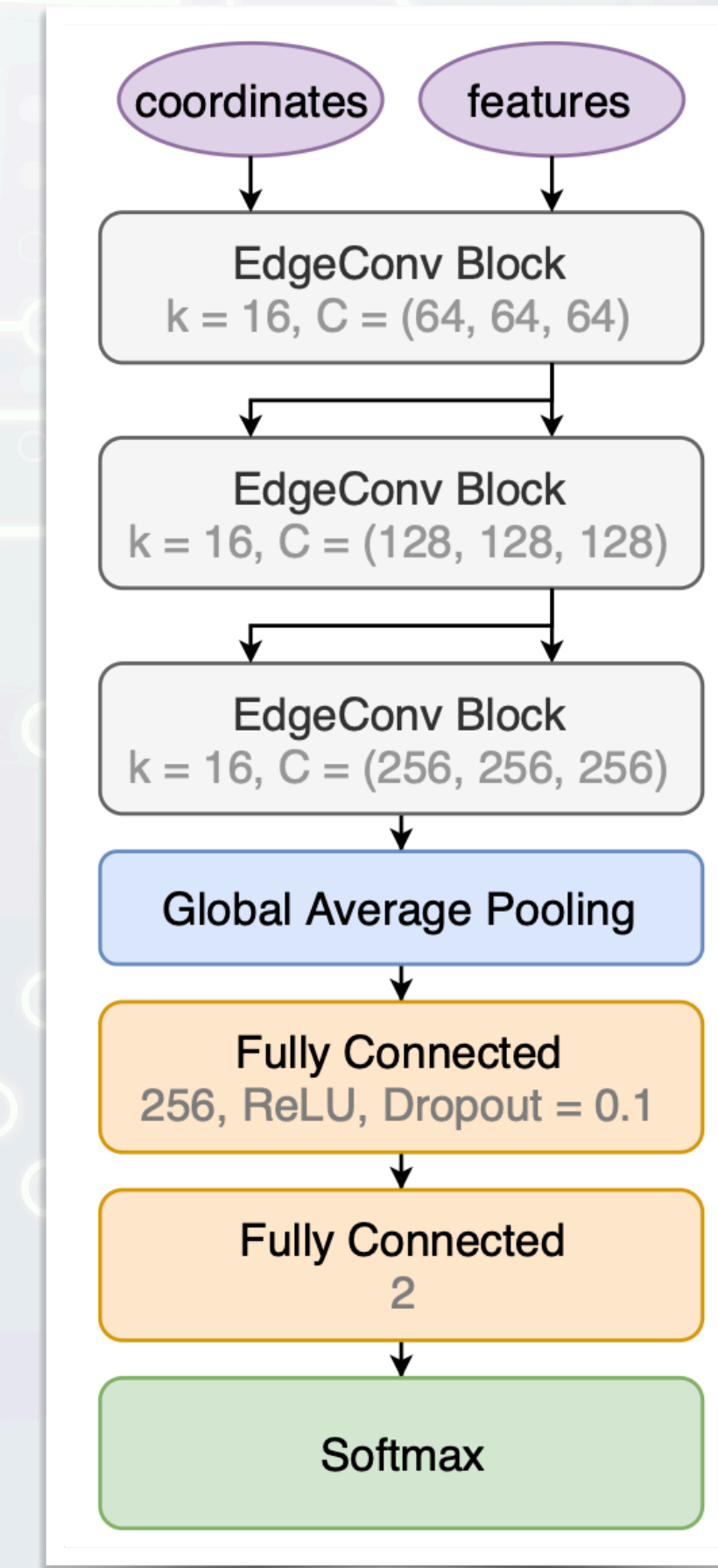
Deep Sets: EFN/PFN
(arXiv 1810.05165)



LSTM (arXiv 1711.09059)



Particle Transformer (arXiv 2202.03772)

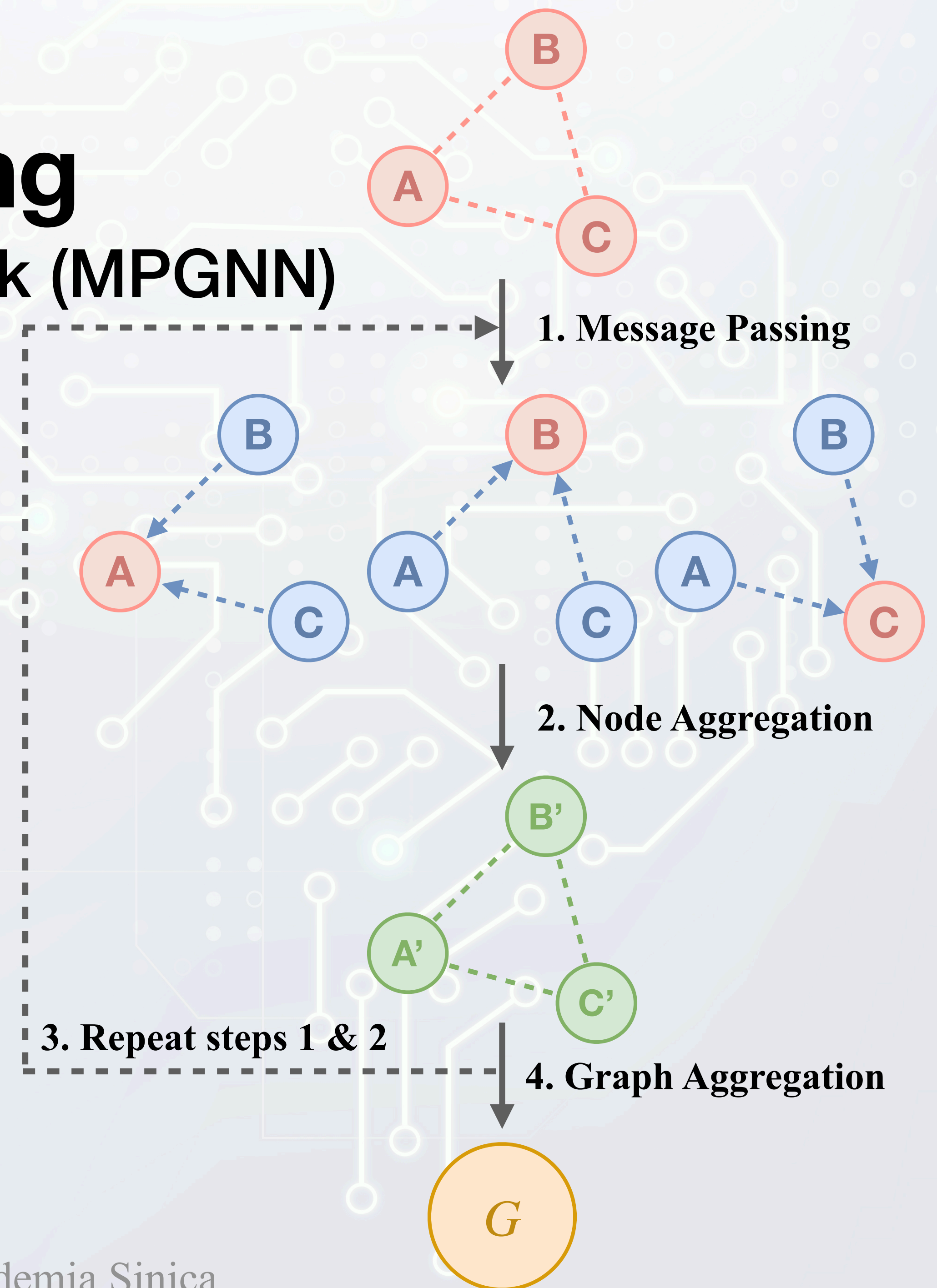


Particle Net
(arXiv 1902.08570)

Classical Machine Learning

Message-Passing Graph Neural Network (MPGNN)

1. **Message Passing**: Compute the information for each particle pair through some parametrized transformation.
2. **Node Aggregation**: Aggregate the transformed information for each particle. Typically element-wise **summation** \iff **permutation-invariant**
3. Repeat step 1 & 2 for several times (optional).
4. **Graph Aggregation**: Aggregate the information of all particles.



Classical Machine Learning

Deep Sets Theorem and MPGNN

- Deep Sets Theorem (arXiv 1703.06114) : A function (model) f is **permutation-invariant** over a

set X (particles) if and only if $f(X) = g \left(\sum_{\mathbf{x}_i \in X} h(\mathbf{x}_i) \right)$ for some suitable transformations g and h .

- The Message-Passing Graph Neural Network (MPGNN) obeys the Deep Sets Theorem, and is usually written as:

$$\mathbf{x}_i^{(k)} = \gamma^{(k)} \left(\mathbf{x}_i^{(k-1)}, \bigoplus_{j \in \mathcal{N}(i)} \phi^{(k)}(\mathbf{x}_i^{(k-1)}, \mathbf{x}_j^{(k-1)}, \mathbf{e}_{ij}) \right)$$

Aggregation function
(MEAN, SUM, MAX, etc.)

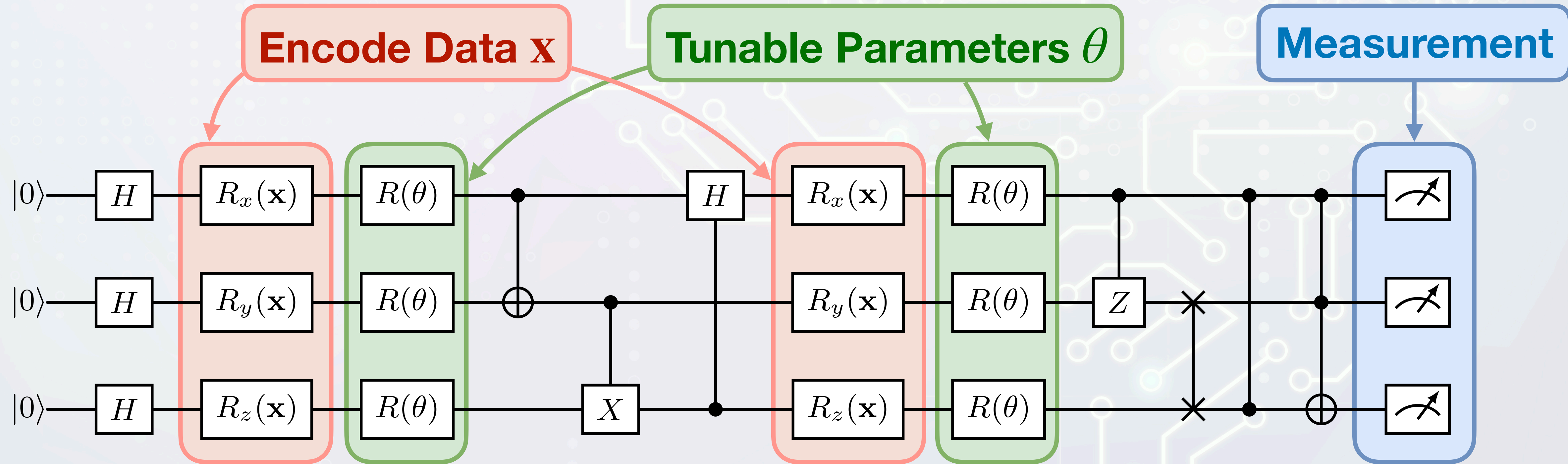
QCGNN

Quantum Complete Graph
Neural Network



Quantum Machine Learning

Variational Quantum Circuit



Updated θ

Gradient Descent

Calculate Loss

Output

QCGNN

Quantum Complete Graph Neural Network

Suppose we have N particles with features $\{\mathbf{x}_i \mid 0 \leq i \leq N - 1\}$. We prepare a quantum circuit with $n_I + n_Q$ qubits where

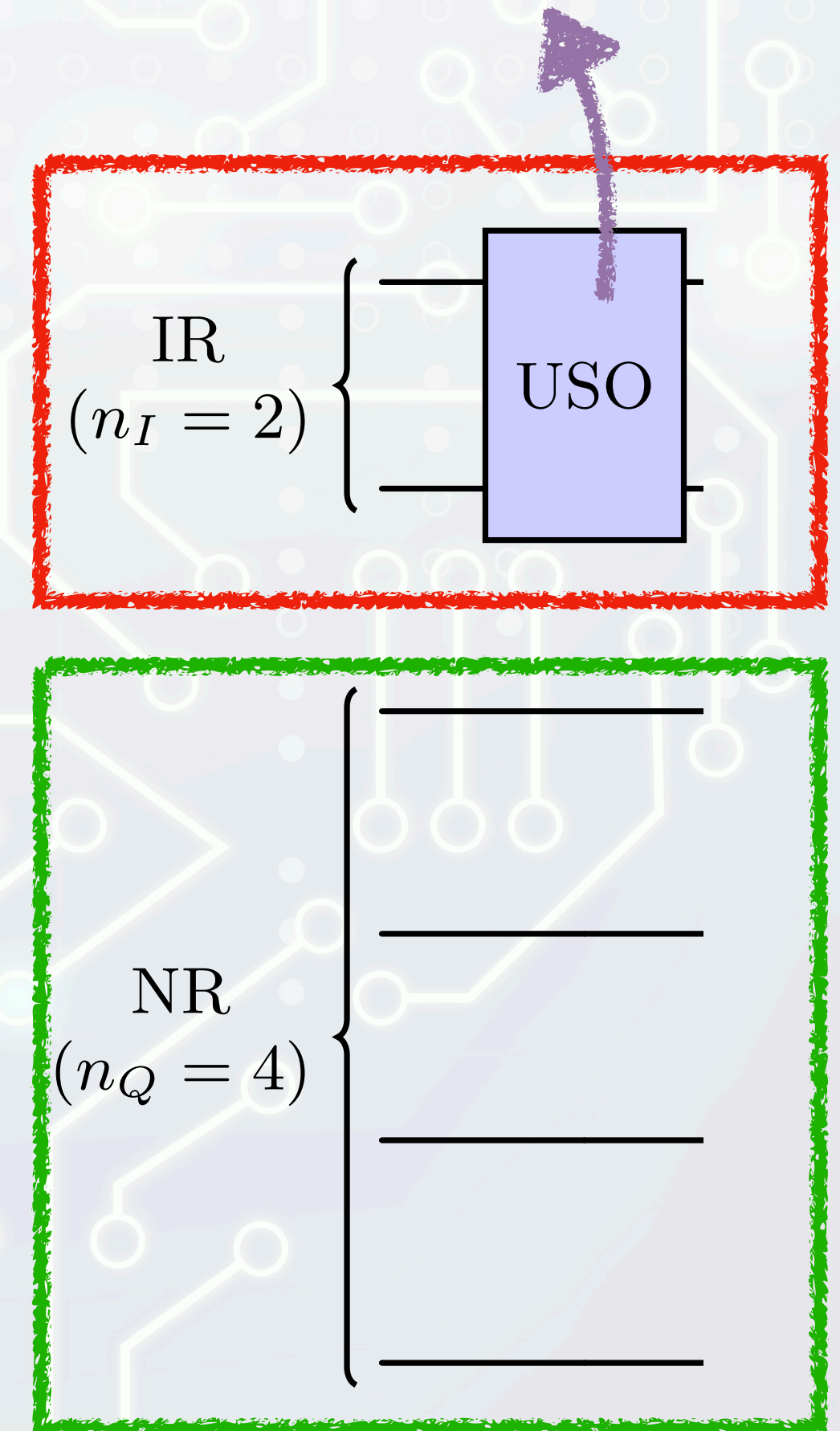
- $n_I = \lceil \log_2 N \rceil$ is the number of qubits in the **index register (IR)**
- n_Q is the number of qubits in the **network register (NR)**

The initial quantum state is initialized as

$$|\psi_0\rangle = \frac{1}{\sqrt{N}} \sum_{i=0}^{N-1} |i\rangle |0\rangle^{\otimes n_Q}$$

If $N = 2^{n_I}$, then we can simply use Hadamard gates. Otherwise, one should use some *Uniform State Oracle* (USO) to prepare the state.

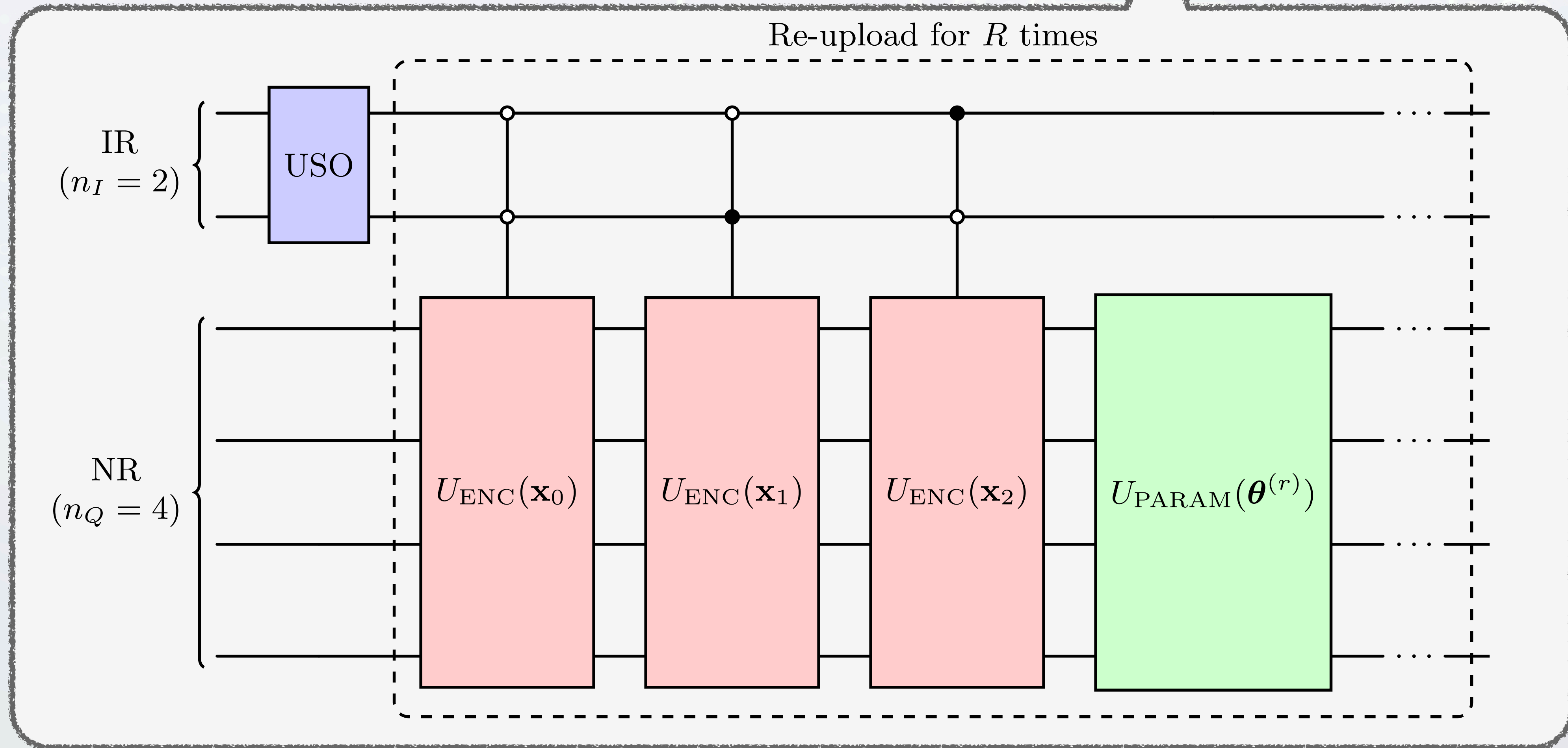
Uniform State Oracle



QCGNN

Quantum Circuit

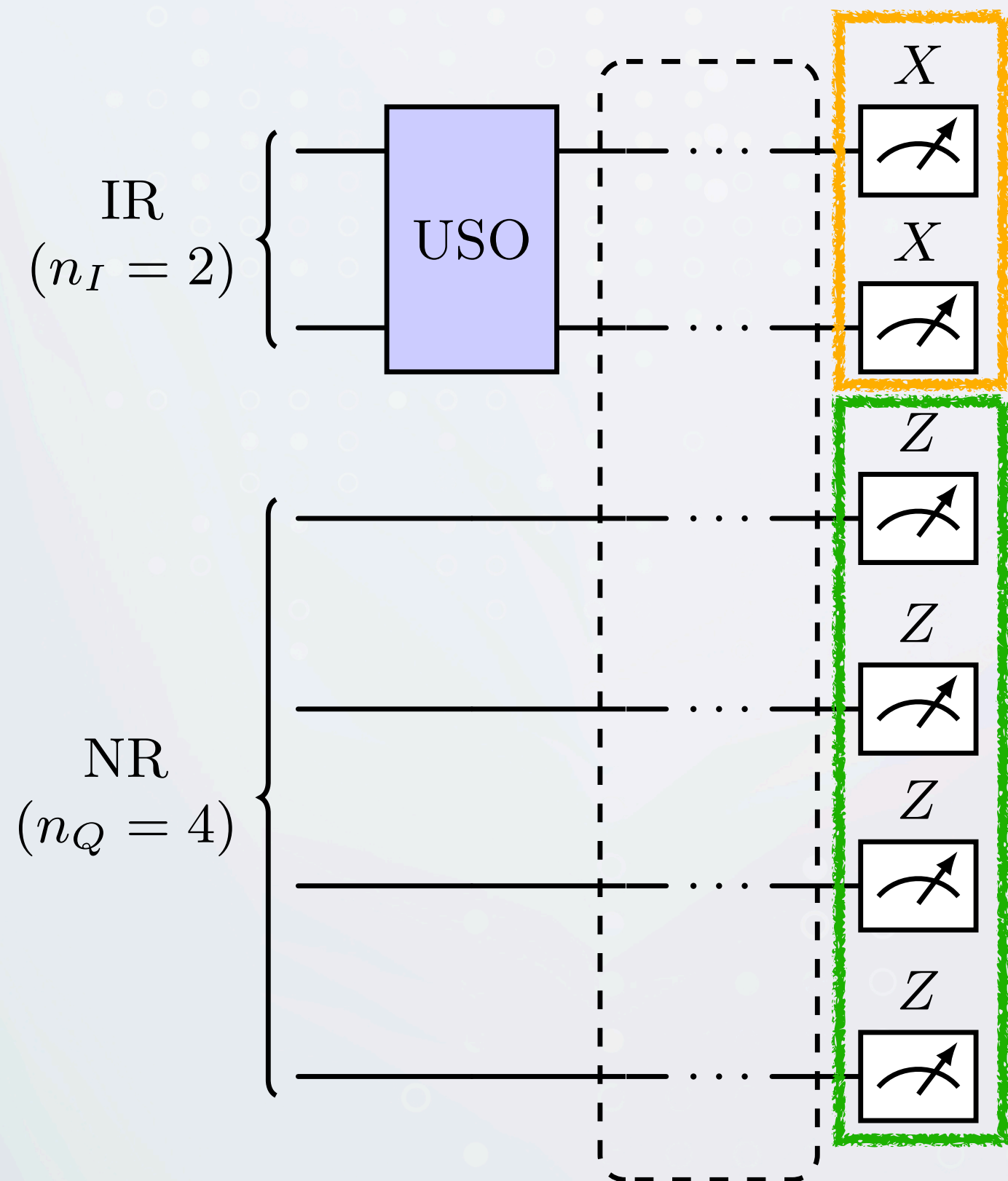
$$|\psi\rangle = \frac{1}{\sqrt{N}} \sum_{i=0}^{N-1} |\mathbf{x}_i, \theta\rangle$$



The QCGNN quantum circuit of a 3-particle jet, with $n_I = 2$ and $n_Q = 4$.

QCGNN

Measurement



The quantum state before measurement is $|\psi\rangle = \frac{1}{\sqrt{N}} \sum_{i=0}^{N-1} |\mathbf{x}_i, \theta\rangle$

Consider a Hermitian matrix J with dimension $2^{n_I} \times 2^{n_I}$ full of ones, i.e.,

$$J = \begin{bmatrix} 1 & \dots & 1 \\ \vdots & & \vdots \\ 1 & \dots & 1 \end{bmatrix} = (I + X)^{\otimes n_I}.$$

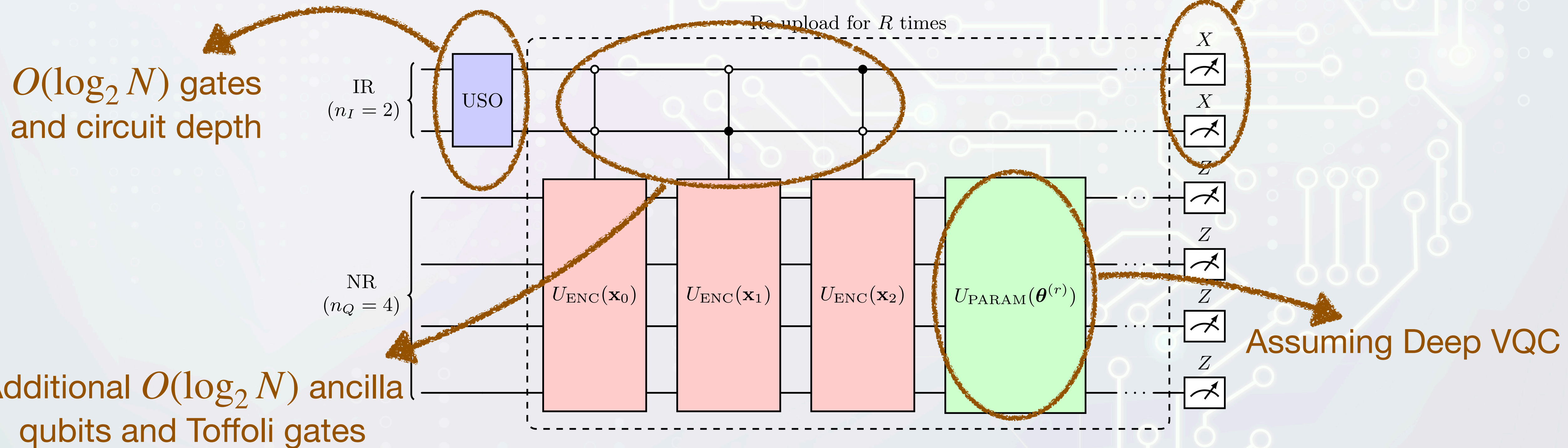
Denote the observables on NR as P , then

$$\langle \psi | J \otimes P | \psi \rangle = \frac{1}{N} \sum_{i < N} \sum_{j < N} \langle \mathbf{x}_i; \theta | P | \mathbf{x}_j; \theta \rangle$$

Similar to MPGNN, with automatic aggregation.

QCGNN

Gate and Computational Complexity



When N is large and the parametrized gates are deep comparing to encoding gates, **QCGNN only needs $O(N)$ computations**, while classical MPGNN requires $O(N^2)$ computations!

Experiments Results

Quantum Simulators & IBMQ



Jet Substructure (CMS 2022 Open Data Workshop)

Jet Dataset

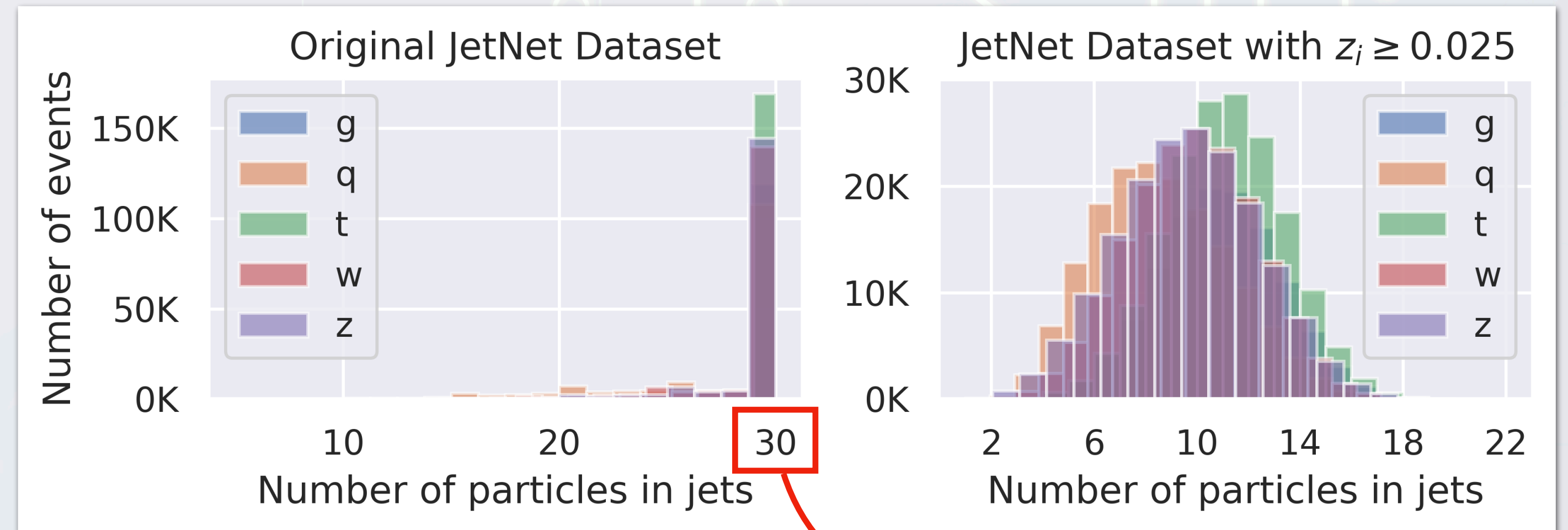
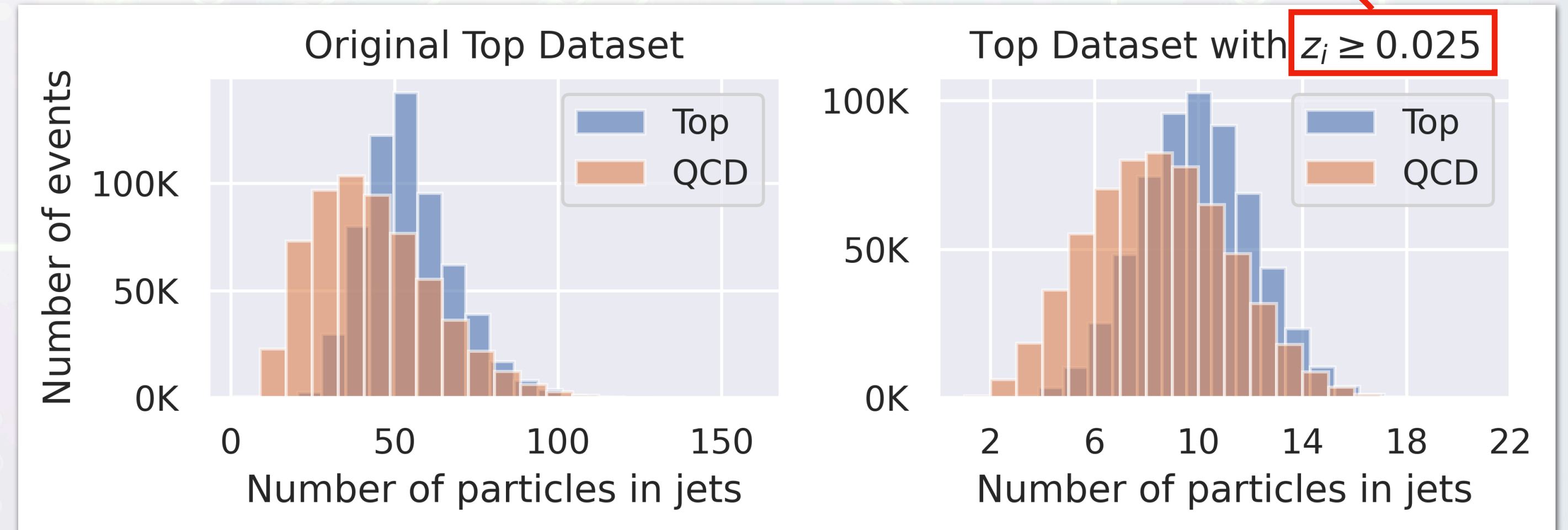
- **Top-Taggers (arXiv 1902.09914)**

- Top v.s. Gluon / Light Quarks
- Jet $p_T \in [550, 650] GeV$
- Pythia / Delphes (ATLAS)
- FastJet with $R = 0.8$

- **JetNet (arXiv 2106.11535)**

- Multi-class $\{g, q, t, W, Z\}$
- Jet $p_T \sim 1 TeV$
- MadGraph / Pythia
- FastJet with $R = 0.8$

$$z_i \equiv \frac{p_{T_i}}{p_{T_{jet}}}$$



Only the 30 highest p_T particles are provided

Training Results

AUC and Accuracy

- Each training process was conducted with 5 different random seeds and 30 epochs.
- Each class has 25K training samples, 2.5K validation samples, and 2.5K testing samples.
- The number of particles of jets lies between 4~16 \implies At most $n_I = 4$ qubits for IR is needed.
- The performance of the state-of-the-art classical models is also presented.

State-of-the-art
classical models

Classical models for
benchmarking

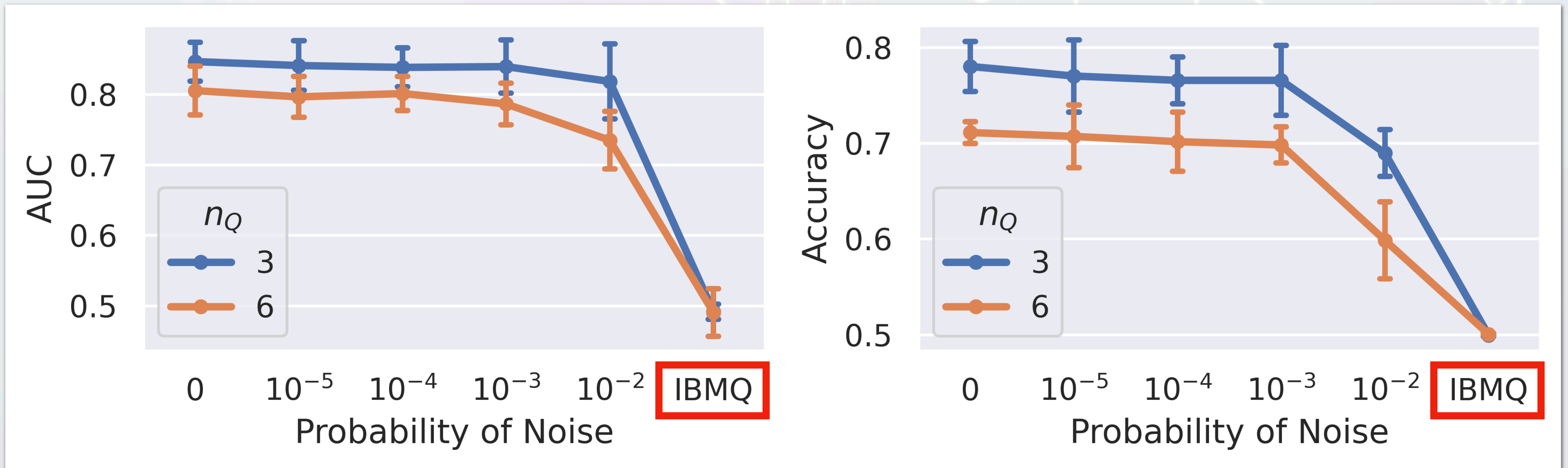
QCGNN with
 $n_Q = 3$ and $n_Q = 6$
(On simulators)

Model	TOP Dataset (2 classes)			JETNET Dataset (5 classes)		
	# params	AUC	Accuracy	# params	AUC	Accuracy
Particle Transformer	2.2M	0.946 ± 0.005	0.868 ± 0.009	2.2M	0.889 ± 0.002	0.656 ± 0.006
Particle Net	177K	0.953 ± 0.003	0.885 ± 0.006	178K	0.896 ± 0.003	0.669 ± 0.004
Particle Flow Network	72.3K	0.954 ± 0.004	0.885 ± 0.005	72.7K	0.900 ± 0.003	0.675 ± 0.005
MPGNN - $n_M = 64$	13K	0.961 ± 0.003	0.896 ± 0.003	13.3K	0.903 ± 0.002	0.683 ± 0.007
MPGNN - $n_M = 6$	255	0.924 ± 0.006	0.866 ± 0.006	323	0.865 ± 0.004	0.615 ± 0.010
MPGNN - $n_M = 3$	126	0.922 ± 0.005	0.864 ± 0.006	194	0.757 ± 0.110	0.475 ± 0.141
QCGNN - $n_Q = 6$	201	0.932 ± 0.004	0.868 ± 0.005	269	0.822 ± 0.003	0.543 ± 0.006
QCGNN - $n_Q = 3$	99	0.919 ± 0.006	0.864 ± 0.005	167	0.796 ± 0.009	0.505 ± 0.014

IBMQ Results

Noise Extrapolation

- The training of QCGNN is done with simulators.
- The **pre-trained** QCGNN is tested on *ibm_brussels*.



IBMQ Results

Runtime of Quantum Gates

- The gate runtime experiment is conducted with two different IBMQ backends for 10 times.
- T_{ENC} and T_{PARAM} are the time for encoding and parametrized gates respectively.

IBMQ Backend	N	T_{ENC}	T_{PARAM}
ibm_nazca	2	2.567	0.209
	4	5.352	0.197
	8	10.551	0.219
ibm_strasbourg	2	2.595	0.217
	4	5.416	0.197
	8	11.085	0.211

Scales as $O(N)$

Constant time $O(1)$

Summary

- In the task of jet discrimination, graph is one of the natural representation. To design permutation-invariant models, graph neural networks have become a popular architecture.
- **We introduce a new quantum model, the **Quantum Complete Graph Neural Network**. If the parametrized gates are deep enough, the cost of QCGNN only scales as $O(N)$, while classical MPGNN requires $O(N^2)$.**
- QCGNN has also been tested on IBMQ real quantum devices. However, due to noise in the quantum circuits, information transmission was unsuccessful.
- As the quantum computers becoming more robust in the future, the potential for quantum advantage of the QCGNN can be studied.

Thanks for your attention! -2-2)

Hypergeometric functions

functions

Special functions

Contour functions

Contour

$\Gamma(z)$
 $\Gamma(z+1) = z\Gamma(z)$
Concatal

$$\frac{\Gamma(z)}{\Gamma(z+1)} = \frac{1}{z}$$

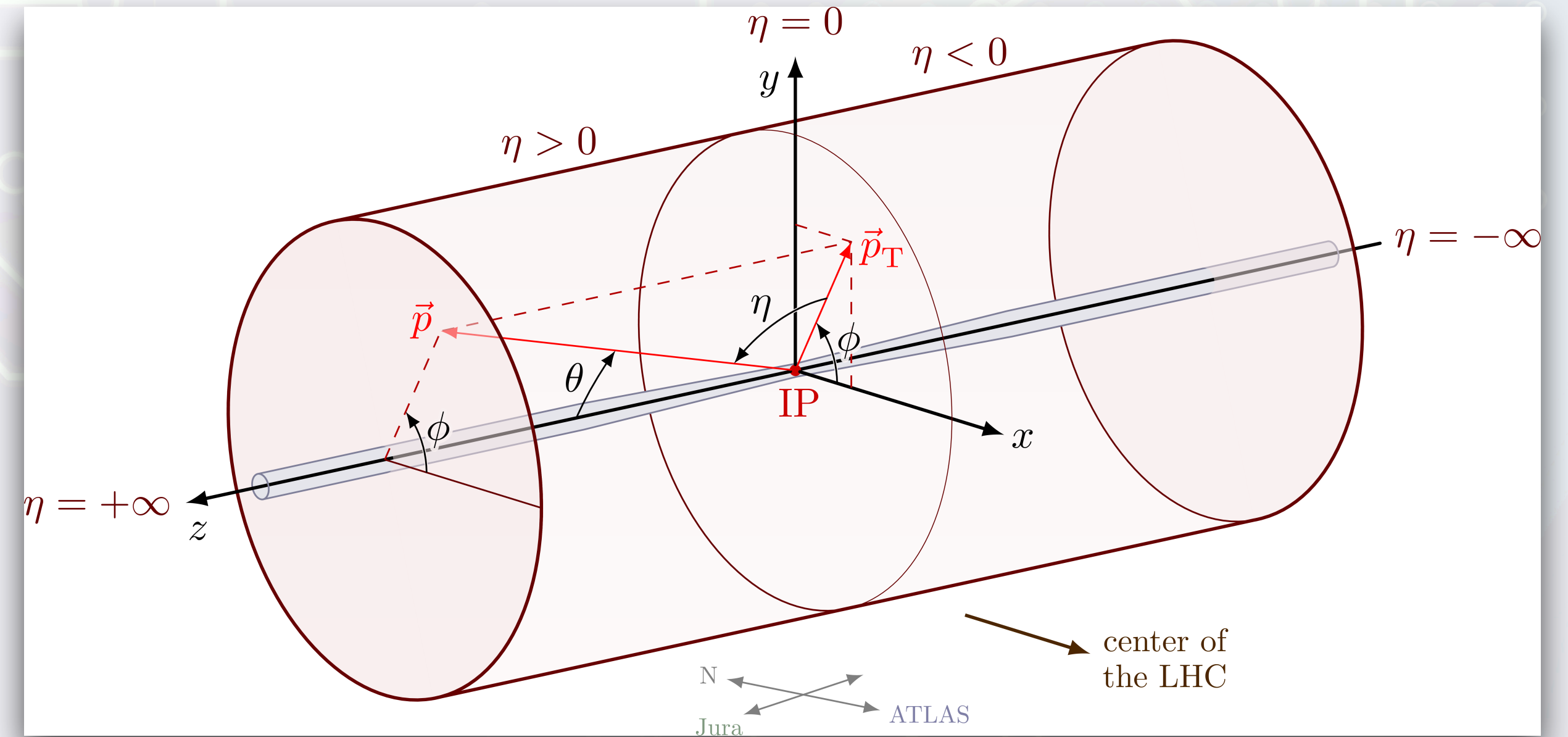


Backup Slides

CMS Coordinate System

The particle flow is defined as

- The transverse momentum $p_T = \sqrt{p_x^2 + p_y^2}$
- The azimuthal angle $\phi = \tan^{-1}\left(\frac{p_y}{p_x}\right)$
- The pseudo-rapidity $\eta = -\ln\left[\tan\left(\frac{\theta}{2}\right)\right]$



CMS Coordinate System by [Izaak Neutelings](#)

In jet analysis, the differences $\Delta\phi$ and $\Delta\eta$ relative to the jets is adopted, since they are **Lorentz invariant** under boosts in z -direction.

Dataset

Top Tagging (arXiv 1902.09914)

2 Data set

The top signal and mixed quark-gluon background jets are produced with using Pythia8 [25] with its default tune for a center-of-mass energy of 14 TeV and ignoring multiple interactions and pile-up. For a simplified detector simulation we use Delphes [26] with the default ATLAS detector card. This accounts for the curved trajectory of the charged particles, assuming a magnetic field of 2 T and a radius of 1.15 m as well as how the tracking efficiency and momentum smearing changes with η . The fat jet is then defined through the anti- k_T algorithm [27] in FastJet [28] with $R = 0.8$. We only consider the leading jet in each event and require

$$p_{T,j} = 550 \dots 650 \text{ GeV} . \quad (1)$$

For the signal only, we further require a matched parton-level top to be within $\Delta R = 0.8$, and all top decay partons to be within $\Delta R = 0.8$ of the jet axis as well. No matching is performed for the QCD jets. We also require the jet to have $|\eta_j| < 2$. The constituents are extracted through the Delphes energy-flow algorithm, and the 4-momenta of the leading 200 constituents are stored. For jets with less than 200 constituents we simply add zero-vectors.

Dataset

JetNet (arXiv 2106.11535)

B JetNet Generation

The so-called parton-level events are first produced at leading-order using MADGRAPH5_aMCATNLO 2.3.1 [51] with the NNPDF 2.3LO1 parton distribution functions [52]. To focus on a relatively narrow kinematic range, the transverse momenta of the partons and undecayed gauge bosons are generated in a window with energy spread given by $\Delta p_T/p_T = 0.01$, centered at 1 TeV. These parton-level events are then decayed and showered in PYTHIA 8.212 [5] with the Monash 2013 tune [53], including the contribution from the underlying event. For each original particle type, 200,000 events are generated. Jets are clustered using the anti- k_T algorithm [54], with a distance parameter of $R = 0.8$ using the FASTJET 3.1.3 and FASTJET CONTRIB 1.027 packages [55, 56]. Even though the parton-level p_T distribution is narrow, the jet p_T spectrum is significantly broadened by kinematic recoil from the parton shower and energy migration in and out of the jet cone. We apply a restriction on the measured jet p_T to remove extreme events outside of a window of $0.8 \text{ TeV} < p_T < 1.6 \text{ TeV}$ for the $p_T = 1 \text{ TeV}$ bin. This generation is a significantly simplified version of the official simulation and reconstruction steps used for real detectors at the LHC, so as to remain experiment-independent and allow public access to the dataset.

Classical ML for Jets

Message Passing GNN

$$f(X) = g \left(\sum_{\vec{x}_i \in X} h(\vec{x}_i) \right)$$

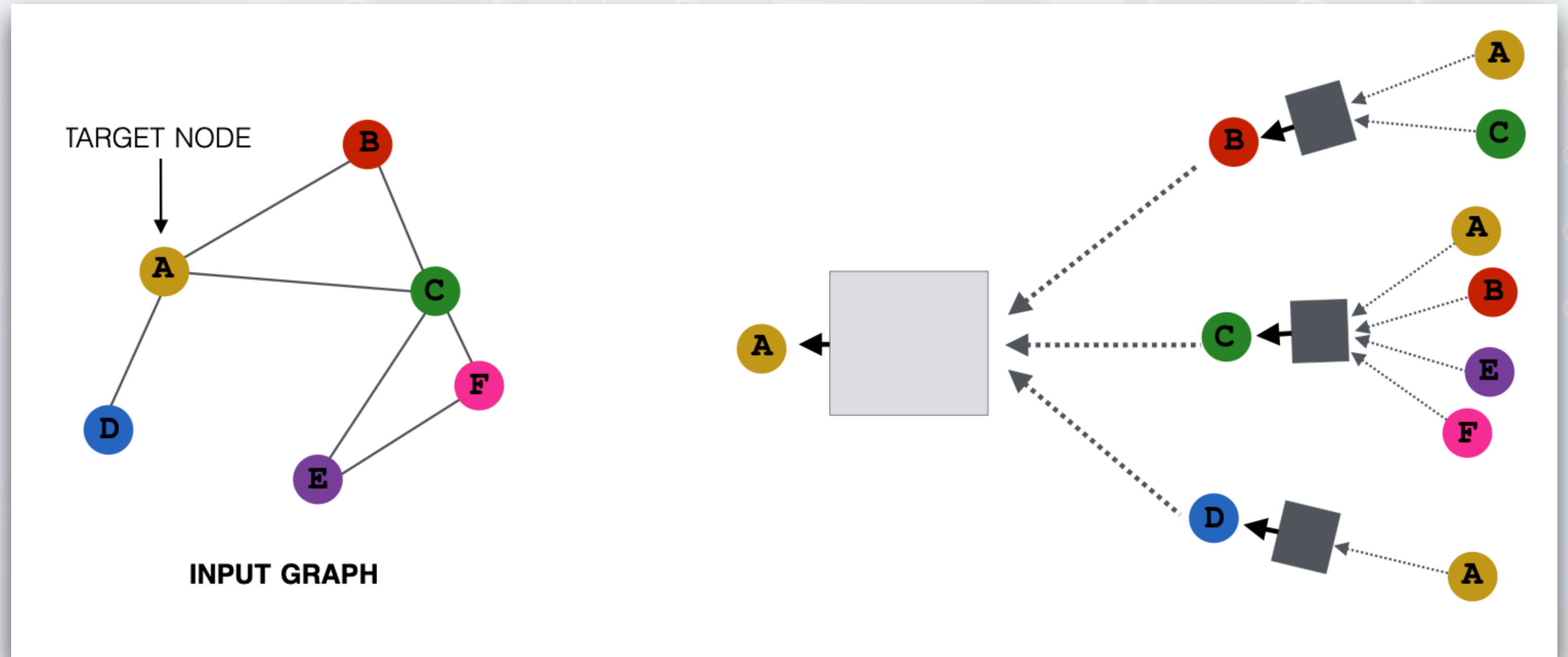


Figure adapted from "Stanford CS224W: Machine Learning with Graphs" by J.Leskovec.

$$\vec{x}_i^{(k)} = \gamma^{(k)} \left(\vec{x}_i^{(k-1)}, \bigoplus_{j \in \mathcal{N}(i)} \phi^{(k)}(\vec{x}_i^{(k-1)}, \vec{x}_j^{(k-1)}, \mathbf{e}_{ij}) \right)$$

k -th update

Aggregation function
(MEAN, SUM, MAX, etc.)

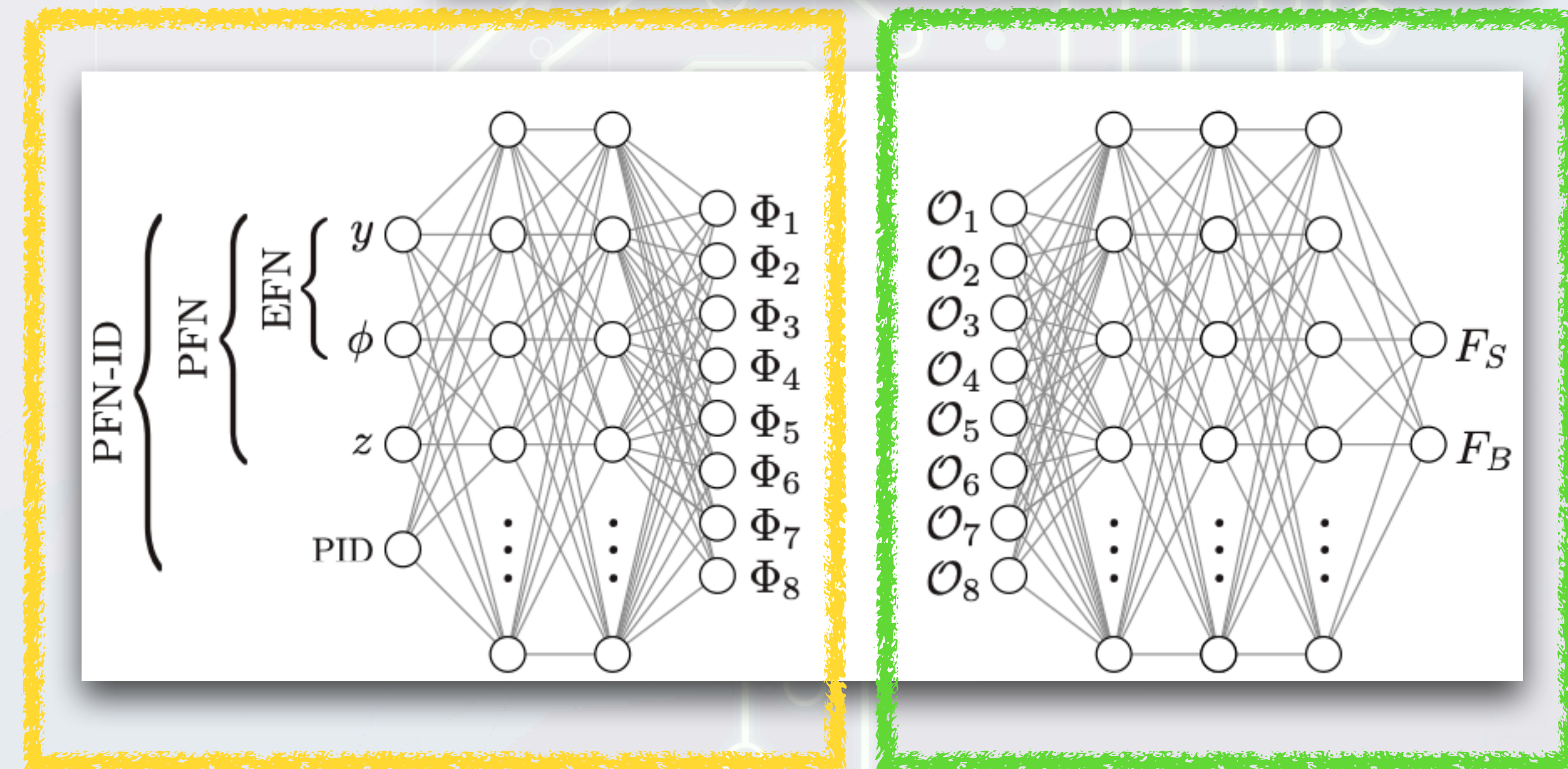
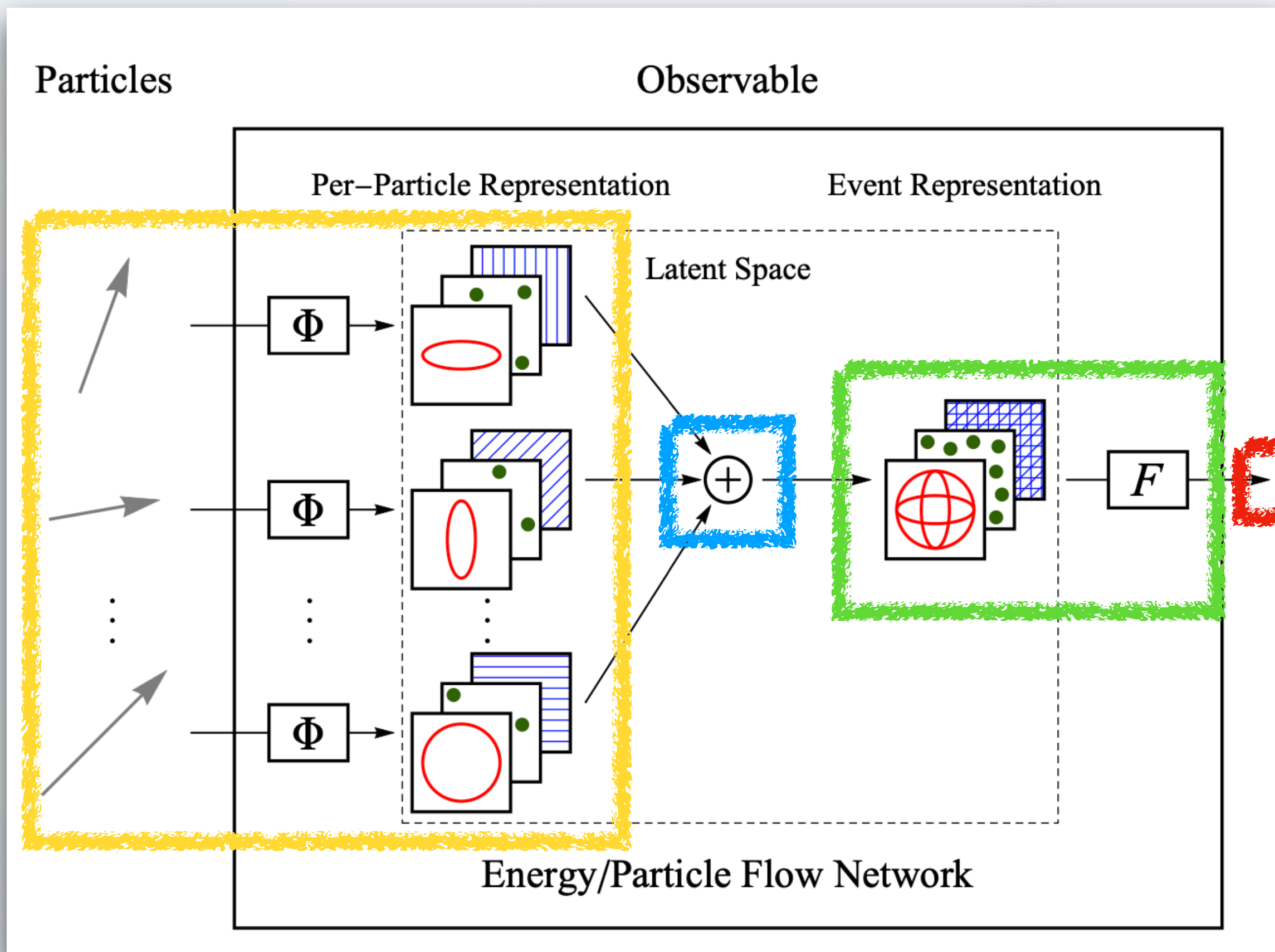
- GCN (arXiv 1609.02907)
- GraphSAGE (arXiv 1706.02216)
- GAT (arXiv 1710.10903)
- EdgeConv (arXiv 1801.07829)

Particle Flow Network

arXiv 1810.05165

Motivated by the *Deep Set Theorem*

$$\mathcal{O}(\{p_1, \dots, p_M\}) = F \left(\sum_{i=1}^M \Phi(p_i) \right)$$



Single Qubit Gates

Rotation Gates

Theorem 4.1: (Z-Y decomposition for a single qubit) Suppose U is a unitary operation on a single qubit. Then there exist real numbers α, β, γ and δ such that

$$U = e^{i\alpha} R_z(\beta) R_y(\gamma) R_z(\delta). \quad (4.11)$$

$$R_x(\theta) \equiv e^{-i\theta X/2} = \cos \frac{\theta}{2} I - i \sin \frac{\theta}{2} X = \begin{bmatrix} \cos \frac{\theta}{2} & -i \sin \frac{\theta}{2} \\ -i \sin \frac{\theta}{2} & \cos \frac{\theta}{2} \end{bmatrix} \quad (4.4)$$

$$R_y(\theta) \equiv e^{-i\theta Y/2} = \cos \frac{\theta}{2} I - i \sin \frac{\theta}{2} Y = \begin{bmatrix} \cos \frac{\theta}{2} & -\sin \frac{\theta}{2} \\ \sin \frac{\theta}{2} & \cos \frac{\theta}{2} \end{bmatrix} \quad (4.5)$$

$$R_z(\theta) \equiv e^{-i\theta Z/2} = \cos \frac{\theta}{2} I - i \sin \frac{\theta}{2} Z = \begin{bmatrix} e^{-i\theta/2} & 0 \\ 0 & e^{i\theta/2} \end{bmatrix}. \quad (4.6)$$

Multi-Qubit Gates

Decomposition of Multi-Controlled Gates

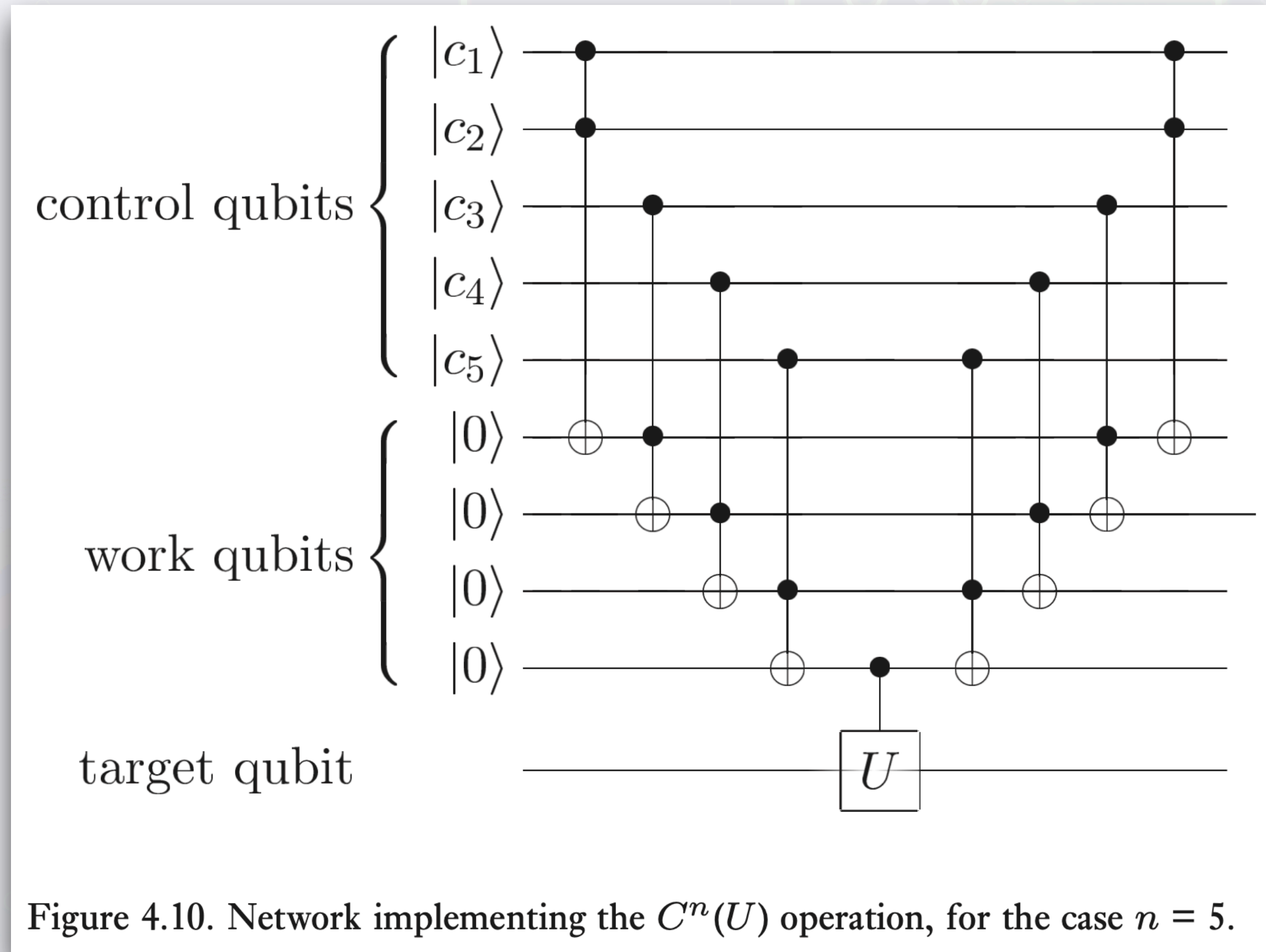


Figure 4.10. Network implementing the $C^n(U)$ operation, for the case $n = 5$.

Adopted from “Quantum Computation and Quantum Information” by N & C.

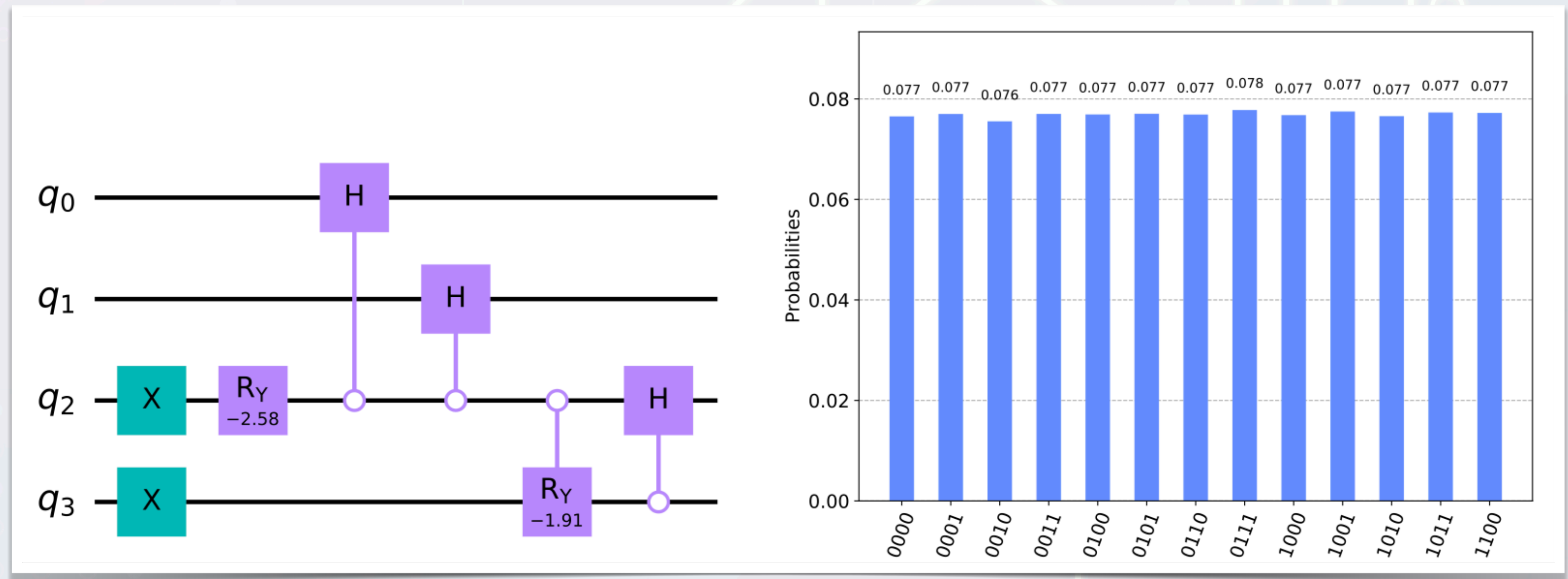
Uniform State Oracle

arXiv 2306.11747

In this paper, we propose an efficient approach for quantum state preparation of uniform superposition state $|\Psi\rangle = \frac{1}{\sqrt{M}} \sum_{j=0}^{M-1} |j\rangle$ that offers a significant (exponential) reduction in gate complexity and circuit depth without the use of ancillary qubits. We show that using only $n = \lceil \log_2 M \rceil$ qubits, the uniform superposition state $|\Psi\rangle$ can be prepared for arbitrary M with a gate complexity and circuit depth of $O(\log_2 M)$.

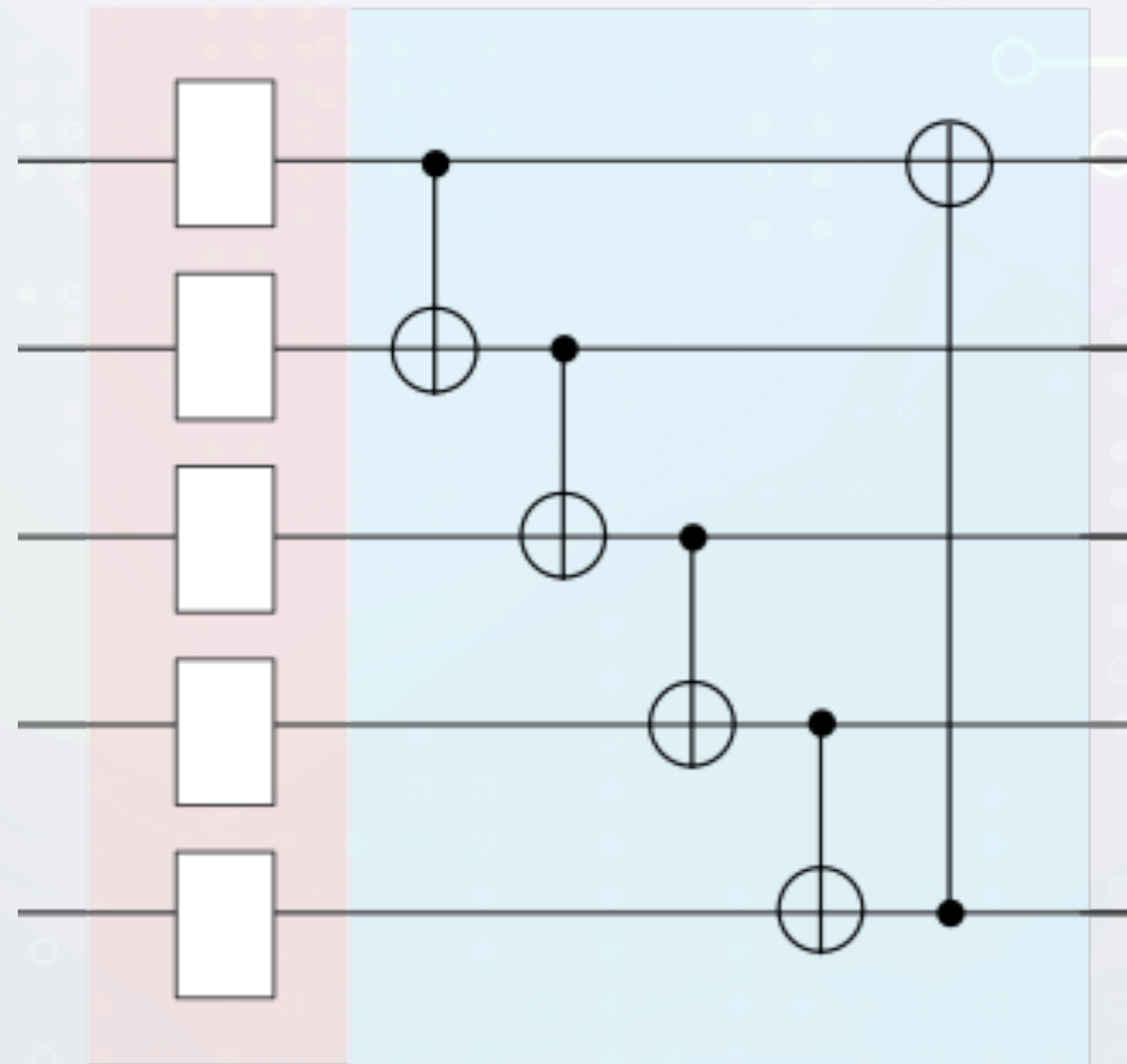
Quantum circuit for generating a 13-basis uniform state:

$$|\psi\rangle = \frac{1}{\sqrt{13}} \sum_{i=0}^{12} |i\rangle$$

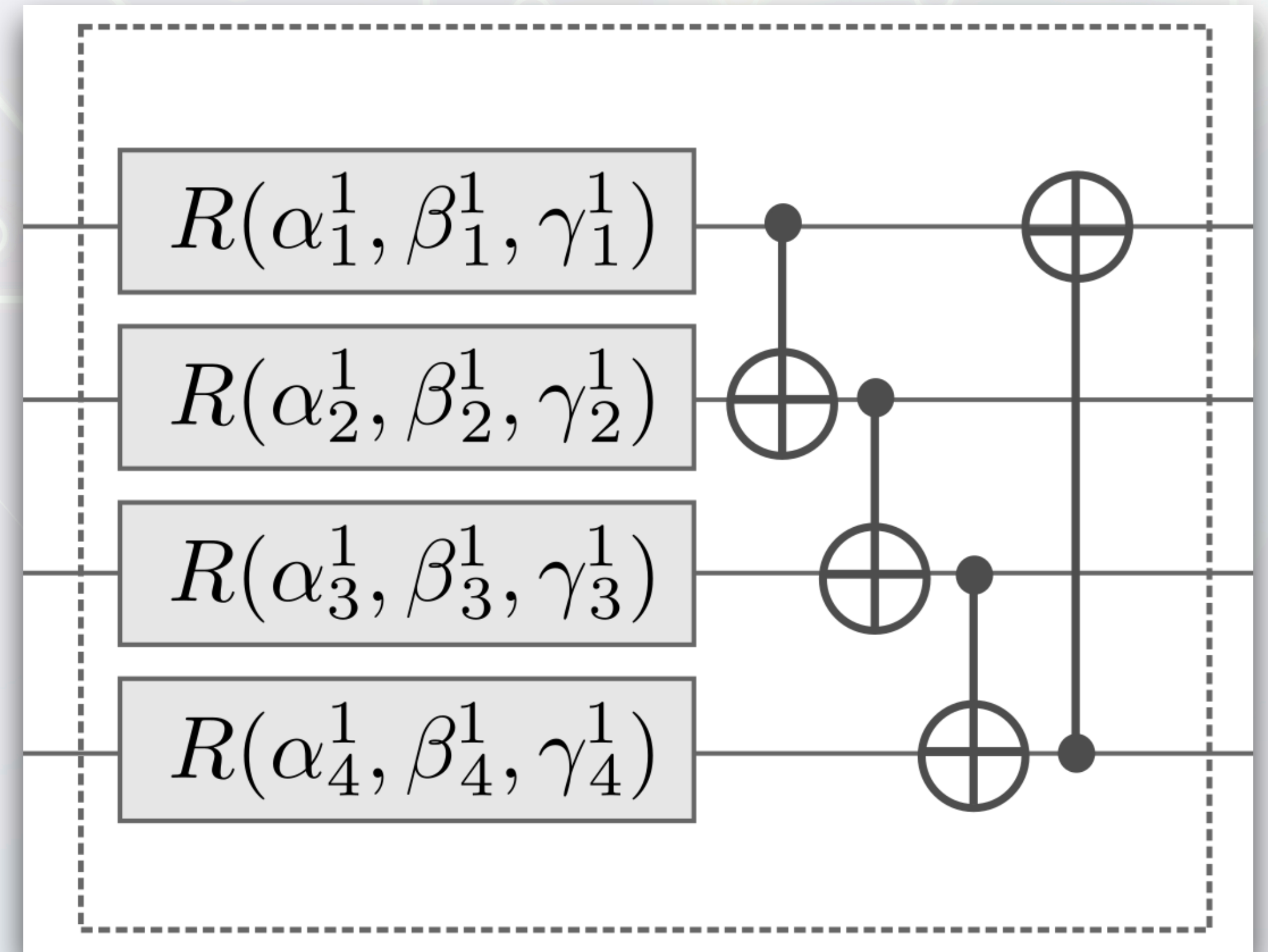


VQC Ansatz

PennyLane

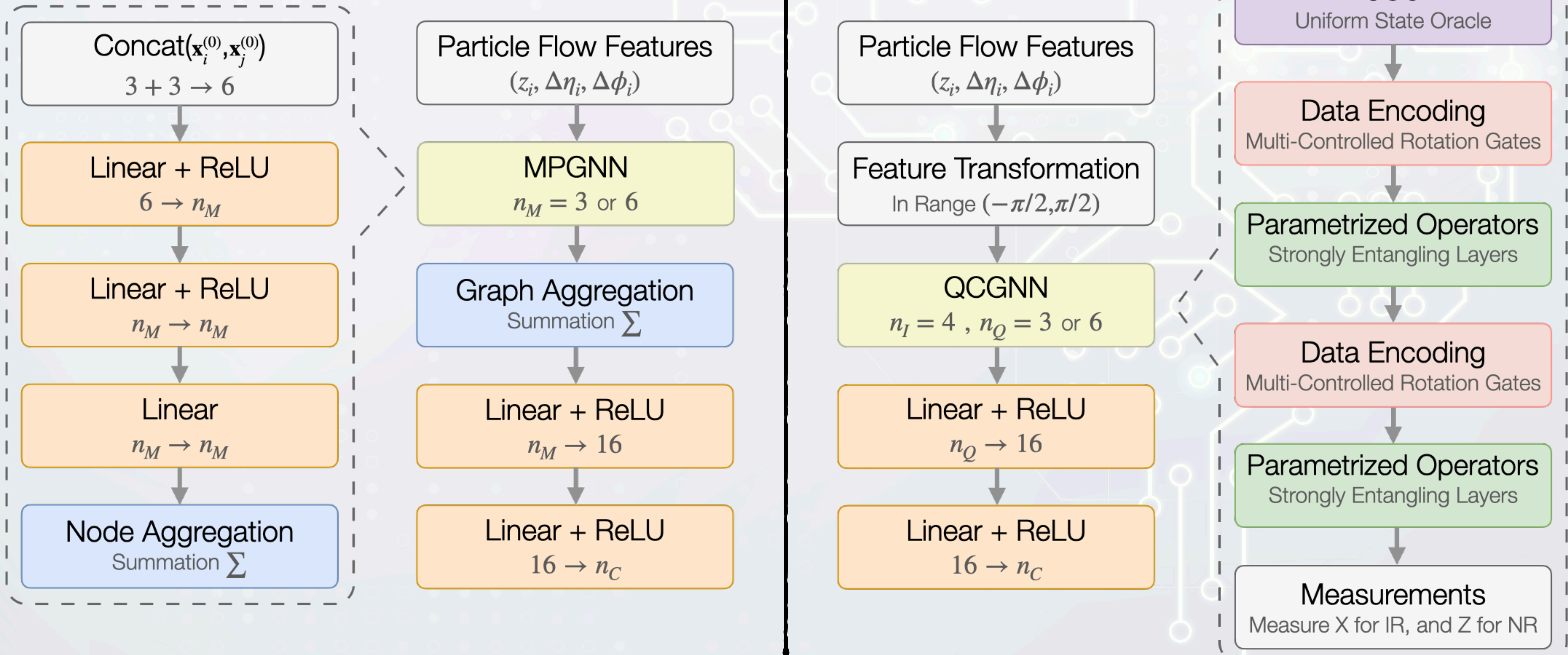


qml.BasicEntanglerLayers



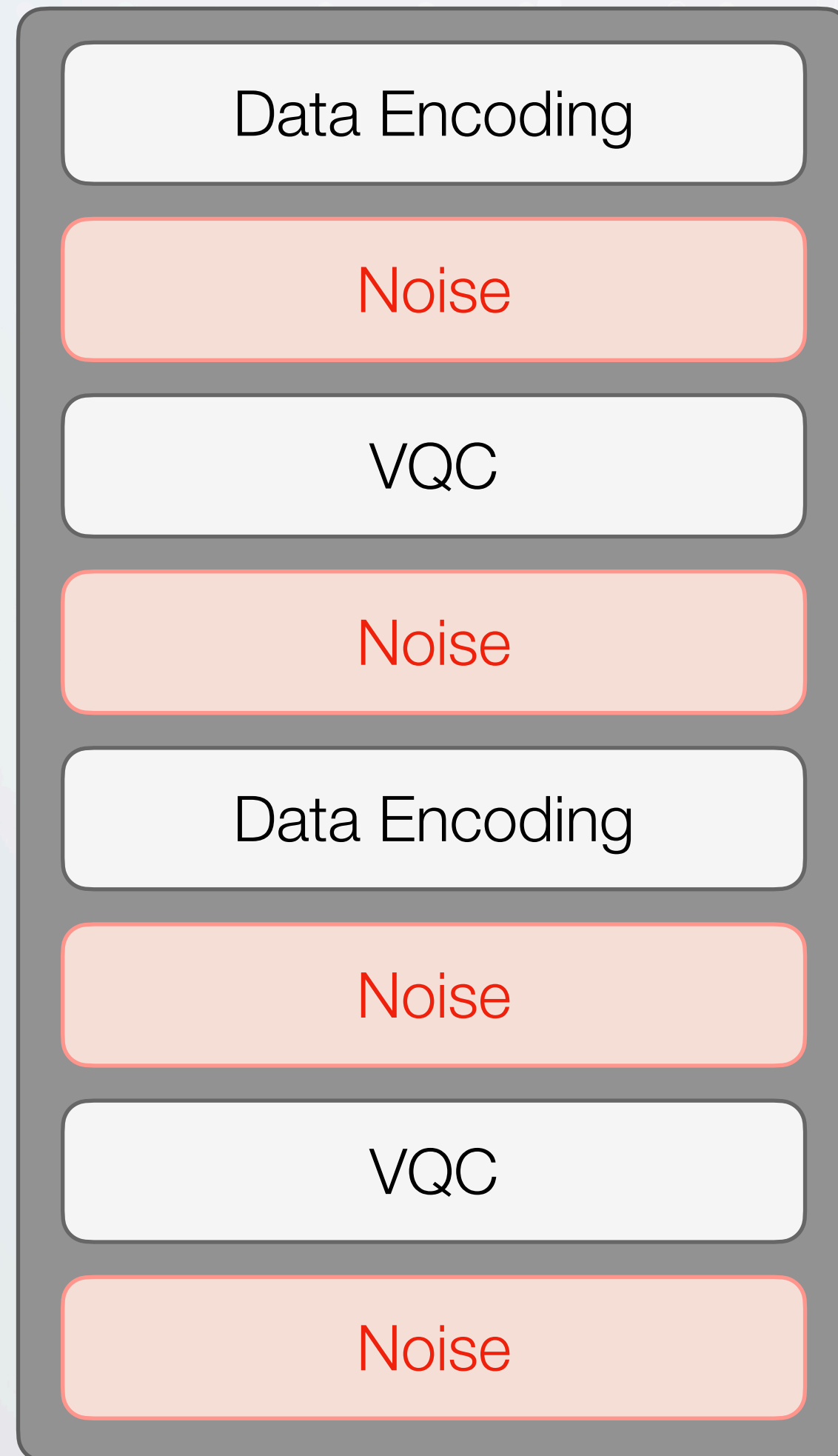
qml.StronglyEntanglingLayers

Model Setup



Noise

Simulated with PennyLane



qml.DepolarizingChannel

$$K_0 = \sqrt{1-p} \begin{bmatrix} 1 & 0 \\ 0 & 1 \end{bmatrix}$$

$$K_1 = \sqrt{p/3} \begin{bmatrix} 0 & 1 \\ 1 & 0 \end{bmatrix}$$

$$K_2 = \sqrt{p/3} \begin{bmatrix} 0 & -i \\ i & 0 \end{bmatrix}$$

$$K_3 = \sqrt{p/3} \begin{bmatrix} 1 & 0 \\ 0 & -1 \end{bmatrix}$$

qml.GeneralizedAmplitudeDamping

$$K_0 = \sqrt{p} \begin{bmatrix} 1 & 0 \\ 0 & \sqrt{1-\gamma} \end{bmatrix}$$

$$K_1 = \sqrt{p} \begin{bmatrix} 0 & \sqrt{\gamma} \\ 0 & 0 \end{bmatrix}$$

$$K_2 = \sqrt{1-p} \begin{bmatrix} \sqrt{1-\gamma} & 0 \\ 0 & 1 \end{bmatrix}$$

$$K_3 = \sqrt{1-p} \begin{bmatrix} 0 & 0 \\ \sqrt{\gamma} & 0 \end{bmatrix}$$

Parameter Shift Rule

arXiv 1905.13311

Gradients of parameterized quantum gates using the parameter-shift rule and gate decomposition

Gavin E. Crooks*

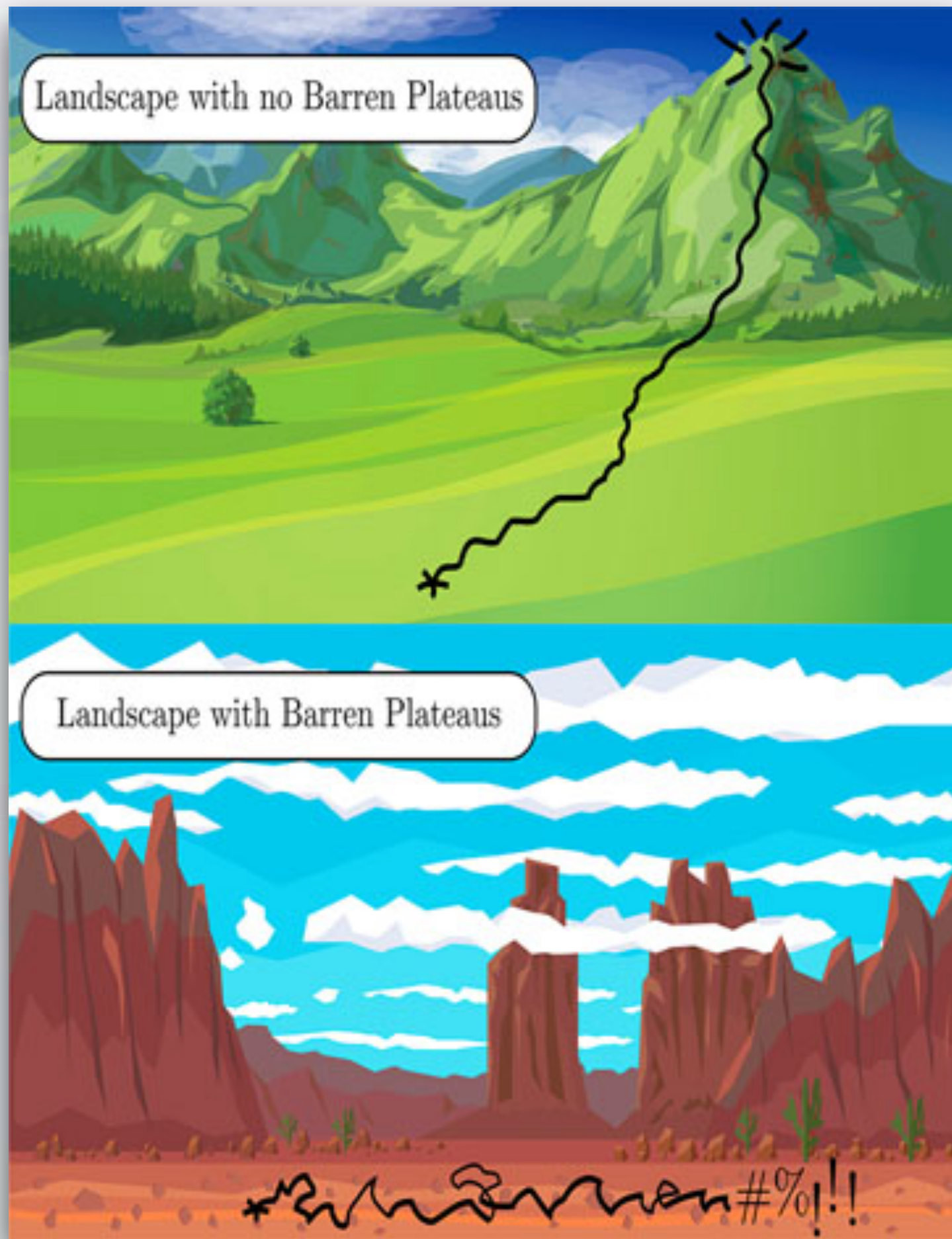
*California Institute of Technology, Pasadena, CA 91125, USA and
Berkeley Institute for Theoretical Sciences, Berkeley, CA 94706, USA*

- Consider a VQC output $f(\theta) = \langle \psi | U_G^\dagger(\theta) A U_G(\theta) | \psi \rangle$, where A is some Hermitian operator of observable and $U_G(\theta) = e^{-ia\theta G}$ with some Hermitian operator G .
- If G has two unique eigenvalues e_0 and e_1 , the gradient can be calculated by

$$\frac{d}{dx} f(x) = r \left[f\left(\theta + \frac{\pi}{4r}\right) - f\left(\theta - \frac{\pi}{4r}\right) \right] \quad \text{with} \quad r = \frac{a}{2}(e_1 - e_0)$$

Barren Plateau

arXiv 2309.09342



$$\text{Var}_{\theta}[\ell_{\theta}(\rho, O)] = \frac{\mathcal{P}_{\mathfrak{g}}(\rho)\mathcal{P}_{\mathfrak{g}}(O)}{\dim(\mathfrak{g})}$$

